

The Physics and Computational Exploration of Zeta and L-functions

Chris King Feb 2016 Genotype 1.1.5

Abstract: This article presents a spectrum of 4-D global portraits of a diversity of zeta and L-functions, using currently devised numerical methods and explores the implications of these functions in enriching the understanding of diverse areas in physics, from thermodynamics, and phase transitions, through quantum chaos to cosmology. The Riemann hypothesis is explored from both sides of the divide, comparing cases where the hypothesis remains unproven, such as the Riemann zeta function, with cases where it has been proven true, such as Selberg zeta functions.

The Conspiracy of Classical Zeta and L-functions

The Riemann zeta function provides the archetype for a vast array of complex functions whose fundamental basis is a deep relationship between products and sums, typified in the Riemann zeta

function by the Euler product formula $\zeta(z) = \sum_{n=1}^{\infty} n^{-z} = \prod_{p \text{ prime}} (1 - p^{-z})^{-1}$ $\text{Re}(z) > 1$, in which a sum of complex exponents of integers is equated with a product over the natural primes.

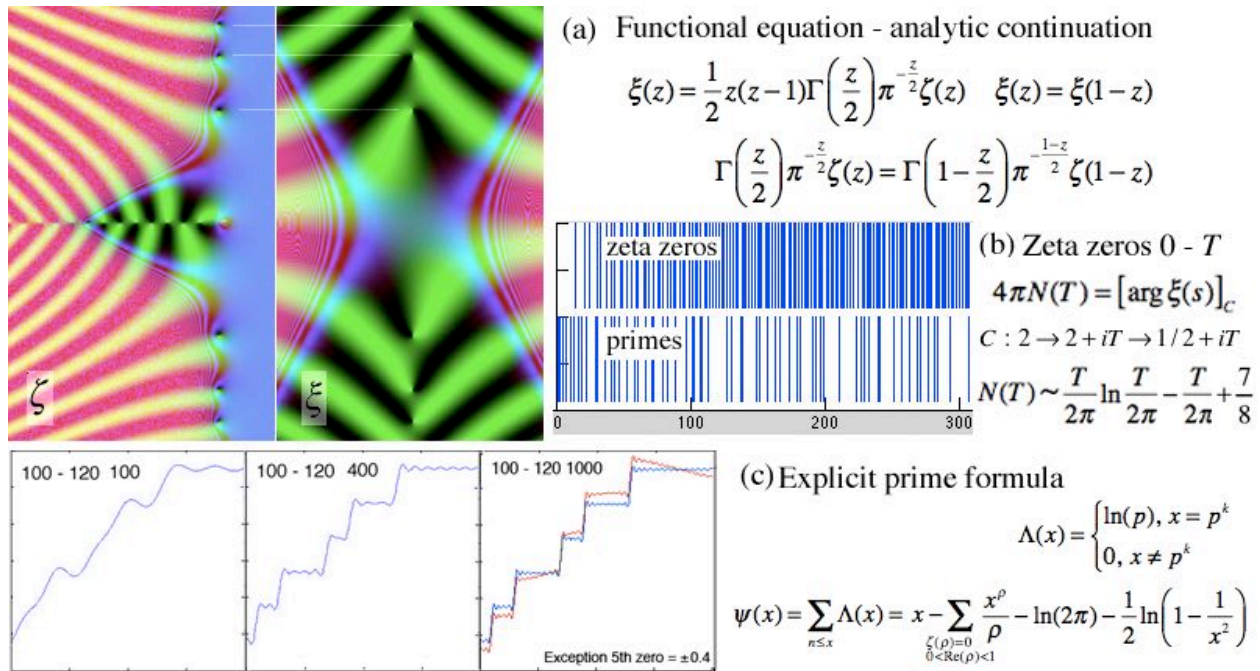


Fig 1: A summary of Riemann's key results. Top left: zeta ζ and xi χ $-30 \leq x \leq 12$ $|y| \leq 27$. Colour scheme on $[0,1]$: **red** logarithmic amplitude using $\log(1+|z|)/(1+\log(1+|z|))$, **yellow/green** $(1-\sin(\angle(z)))/2$, **blue** $(1-\cos(\pi(|z|)))/2$ with first peak at 1. (a) A functional equation giving an analytic continuation via the xi function, which shares the same non-trivial zeros. (b) A distribution for the non-trivial zeros, noting they probably all lie on $x = 1/2$. (c) He uses the zero distribution in the form of an integral transform to define a prime counting function $\pi(x) \sim li(x)$ the logarithmic integral. Here, von Mangoldt's explicit formula is used, because it is easier to compute and shows the prime counting function is a type of Fourier transform of the zeros, which depends on the RH, because an off critical zero (split in pairs because of the symmetry in (a)) disrupts the prime distribution function **blue**, as shown in **red**.

Bernhard Riemann exposed the core secrets of this enigmatic function, scribbled in long-hand, in four almost illegible pages in 1859 (see fig 11), containing three key results, summarized in fig 1: (a) An analytic continuation of the function to the entire complex plane, (b) the distribution of the zeros for increasing imaginary values, and (c) using the zeros to deduce a formula for a prime counting function. In passing he notes the Riemann hypothesis (RH) that "it is probable" that the

unreal zeta zeros lie on $x = 1/2$, lamenting "Certainly one would wish for a stricter proof here; I have meanwhile temporarily put aside the search for this after some fleeting futile attempts".

Since then, the tantalizing symmetry of the roots as an explanation for the prime distribution has remained a mathematical nemesis, despite the efforts of genius minds to bring to bear every device, from quantum eigenfunctions of Hermitian operators with real eigenvalues locking to the critical line, to ultimately esoteric branches of abstract mathematics, with the only definitive result since being that of Albert Ingham, who showed that $\psi(x) = x + O(x^\theta \ln^2 x)$, $\pi(x) = \text{li}(x) + O(x^\theta \ln x)$, for $\theta = \sup(\text{Re}(\rho))$ using similar techniques to Riemann, establishing that the supremum of the real parts of the zeros define the asymptotic fluctuations of the primes and vice versa, raising the question of whether zeta is the key to unlocking the primes, or merely an expression of their underlying consistency, being as close to evenly distributed as they can be given that they can't.

Of course there have been many intriguing results along the way. We know for example that at least 2/5ths of the non-trivial zeros are simple and lie on the critical line (Conrey 1989). The zeros have been explored computationally and have been shown to lie on the line to experimental error up to values as large as 10^{22} (Odlyzko 2001). We can tell that $\arg(\zeta(1/2 + it))$ governing fluctuations in the number of zeros to t grows extremely slowly with t in the average as $\sim (\ln(\ln(t)))^{1/2}$, so that major fluctuations in the zeros might not emerge with the large numbers so far computed. Other properties of the zeta function, such as changes in the topology of $\text{real}(\zeta(s))=0$, emerge only with moderately large numbers.

Alternatively one can look for fluctuations in the primes themselves. RH is equivalent to the conjecture that the prime counting function $\pi(x) = \text{Li}(x) + O(x^{1/2+\varepsilon})$, $\forall \varepsilon > 0$, where

$\text{Li}(x) = \int_2^x \frac{dt}{\log t}$. In a classic result closely related to the zeta zeros, Littlewood proved that

$\pi(x) - \text{li}(x)$, $\text{li}(x) = \int_0^x \frac{dt}{\log t}$ changes sign infinitely often, although the difference is negative for

all calculated primes. Skewes' (1933) bound for a change of sign of $10^{10^{34}}$ assuming RH and $10^{10^{963}}$ not assuming it (1955), shows such changes could occur far beyond numbers so far computed. Although lower computer bounds of 1.398×10^{316} , where there are at least 10^{153} consecutive such integers near this value without assuming RH have been established, these are still astronomical by comparison with the known zeta zeros, so further anomalies in zeta zeros could appear.

A second form of RH is that: $M(n) = \sum_{k=1}^n \mu(k) = O(n^{1/2+\varepsilon}) \forall \varepsilon > 0$, where

$\mu(n) = \begin{cases} (-1)^k, & n \text{ has } k \text{ distinct prime factors of multiplicity } 1 \\ 0 & \text{otherwise} \end{cases}$. This is minimal, as Mertens'

conjecture that $|M(n)| < n^{1/2}$, effectively relaxing ε to zero, has been disproved by Odlyzko & te Riele (1985) without stating the number at which a violation would occur. Estimates lie between 10^{14} and $e^{1.59 \times 10^{40}}$ (Kotnik & te Riele 2006). Estimates of the growth of $m(n)$ lie between $(\log \log \log n)^{5/4}$ and $(\log \log n)^{1/2}$ again suggesting huge numbers for a counterexample. The highest known value of $M(n) / n^{1/2}$ is 0.570591 for $n = 7766842813$.

RH is equivalent to the statement that $\sum_{n=1}^{\infty} \frac{\mu(n)}{n^s}$ is convergent for $\text{Re}(z) > 1/2$, since the convolution $(f * g)(n) = \sum_{d|n} f(d)g(n/d)$ of the Dirichlet series coefficients

$$\mu * 1 = \varepsilon, \varepsilon(n) = \begin{cases} 1, & n = 1 \\ 0, & n > 1 \end{cases} \text{ shows that } \sum_{n=1}^{\infty} \frac{\mu(n)}{n^s} \zeta(s) = 1, \text{ and therefore } \sum_{n=1}^{\infty} \frac{\mu(n)}{n^s} = \frac{1}{\zeta(s)}.$$

In his AMS review, Brian Conrey (2008) notes that a major difficulty in trying to construct a proof of RH through analysis is that the zeros of [the various zeta] and L -functions *behave so much differently from zeros of many of the special functions we are used to seeing in mathematics and mathematical physics. For example, it is known that the zeta-function does not satisfy any differential equation* [although paradoxically zeta-function universality states that there exists some location on the critical strip that approximates any holomorphic function arbitrarily well]. *It is my belief that RH is a genuinely arithmetic question that likely will not succumb to methods of analysis. There is a growing body of evidence indicating that one needs to consider families of L -functions in order to make progress on this difficult question. However in the same paper he concedes: "There is a growing body of evidence that there is a conspiracy among L -functions – a conspiracy that is preventing us from solving RH".*

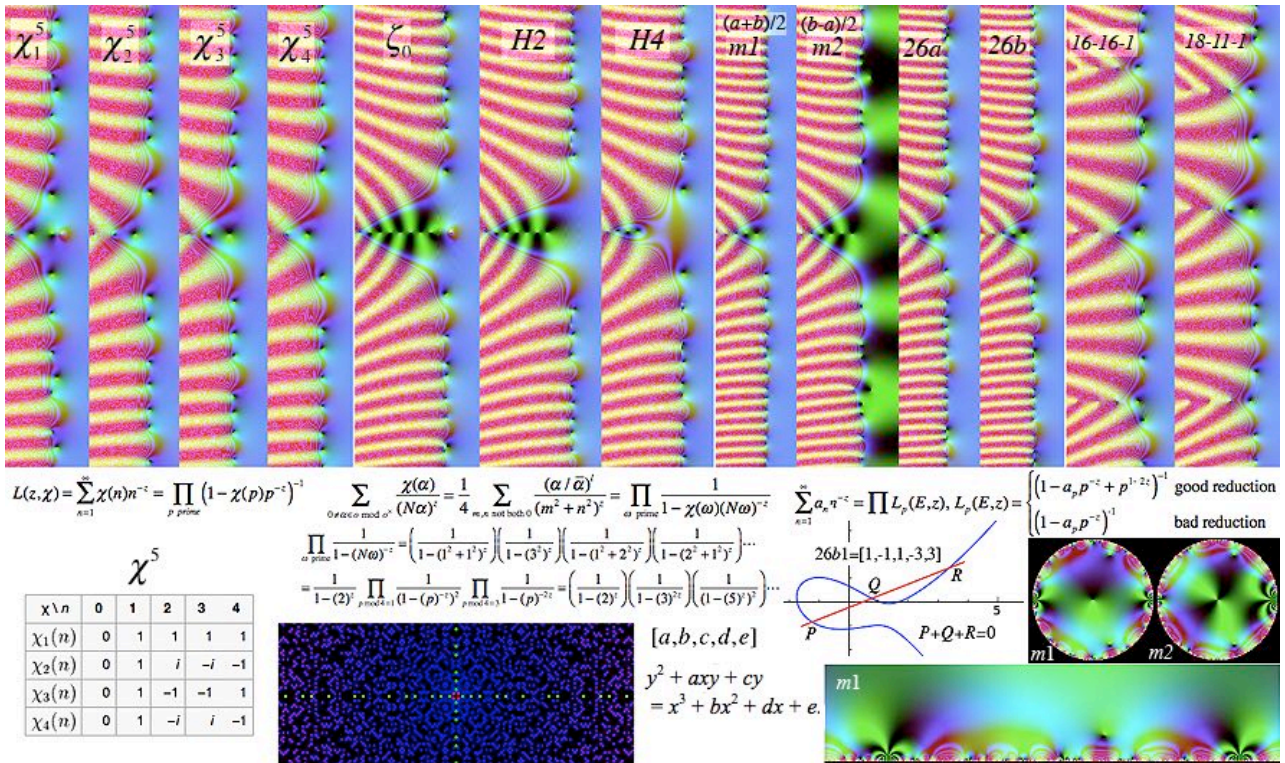


Fig 2: A variety of zeta and L -functions from left to right depicted using the authors open source Mac application RZViewer (King 2009b): The four Dirichlet L -functions mod 5, with their cyclic characters defined below, the Dedekind zeta function and two Hecke L -functions of the Gaussian integers, two echelon modular form L -functions for $n=26$, with their associated elliptic curve L -functions, and two third degree Mass form L -functions incorporating $GL(3)$ elements. Each has an Euler product, and an analytic continuation to \mathbb{C} via the functional equations listed in Appendix 2. The product over Gaussian primes illustrated lower centre for the Dedekind zeta is expanded in terms of the natural primes to show the natural primes underlie the Dedekind and Hecke examples. Lower centre: The distribution of the Gaussian primes of 3 types [red $(\pm 1 \pm i)$, green $(0, \pm 4n+3)$ $(\pm 4n+3, 0)$, blue/magenta $(m^2+n^2) = 4n+1$: $4n+k$ prime] In a similar manner the natural primes underlie the Euler products defining elliptic curve, modular form and Maass form L -functions. Lower right the modular forms illustrated above are portrayed in the unit disc and upper half-plane using power series and Fourier transforms of the Dirichlet series coefficients.

We will now explore the diversity of such functions to see why this may be the case, several of which are illustrated in fig 2. The essential reason is that, although these functions were perceived to be unrelated and not necessarily invoking RH, in their fundamental generating properties, they are all singing the same song – that of the distribution of the natural primes.

The two central features defining classical zeta and L -functions are (1) an Euler product equation based on the natural primes, defining a Dirichlet series and (2) an analytic continuation involving one or more gamma functions. These are the two key axiomatic attributes of the 'Selberg Class' characterizing such functions.

Key in defining each function is the product RHS of the Euler product equation. In every case this is a formula dependent on the natural primes, defining the process generating the function. The Dirichlet series on the LHS is a summation version of the product, which is amenable to being transformed by gamma functions, using the Mellin integral transform, to produce a functional equation that provides an analytic continuation over the complex plane.

Riemann's zeta and the Dirichlet L -functions

Closely associated with Riemann's zeta are the Dirichlet L -functions, illustrated in fig 2 for $n = 5$. The character $\chi_2^5(n)$ consists of the elements of the group of residues modulo 5, modifying both the Euler product and the coefficients of the Dirichlet series:

$$L(z, \chi) = \sum_{n=1}^{\infty} \chi(n) n^{-z} = \prod_{p \text{ prime}} (1 - \chi(p) p^{-z})^{-1} \text{ where } \chi(n), n = 0, \dots, k-1 \text{ is a Dirichlet character.}$$

A Dirichlet character is any function χ from the integers to the complex numbers, such that:

- 1) *Periodic*: There exists a positive integer k such that $\chi(n) = \chi(n+k)$ for all n .
- 2) *Relative primality*: If $\gcd(n, k) > 1$ then $\chi(n) = 0$; if $\gcd(n, k) = 1$ then $\chi(n) \neq 0$.
- 3) *Completely multiplicative*: $\chi(mn) = \chi(m) \chi(n)$ for all integers m and n .

Dirichlet L -functions have a functional equation invoking the conductor N , the characters and their conjugates:

$$N^{s/2} \pi^{-(s+a)/2} \Gamma\left(\frac{s+a}{2}\right) L(s, \chi) = N^{(1-s)/2} \pi^{-((1-s)+a)/2} \Gamma\left(\frac{(1-s)+a}{2}\right) L(1-s, \bar{\chi})$$

The Dirichlet series, provides the basis for developing a functional equation based on Mellin integral transforms, which behave like Fourier transforms in the imaginary direction, and we thus get an analytic continuation expressing the fact that, underlying both the product and sum formulae, which are convergent only for $\text{Re}(z) > 1$, is the ghost in the machine – the underlying analytic function containing the zeroes.

The series remains merely a cypher for the product. While it is not immediately obvious why

the series $1 + \frac{i}{2^z} - \frac{i}{3^z} - \frac{1}{4^z} + \frac{1}{6^z} + \frac{i}{7^z} - \frac{i}{8^z} - \frac{1}{9^z} + \dots$ should converge to an L -function

potentially obeying RH, given the lack of numerical relationships between 2, 7 or 3, 8 except that they both give the same remainder on division by 5, it is clear that the product

$\prod_{p \text{ prime}} (1 - \chi(p) p^{-z})^{-1}$ is distributing the residues mod 5 cyclically over all the other primes.

If the primes are distributed in a non-mode-locked manner, as is clear from the Farey sequences, then radiating these coefficients over the other primes is as likely to obey RH as

the string of 1's of the Riemann zeta function.

The Farey sequences appear in a third manifestation of RH (Franel and Landau 1924). These consist of all fractions with denominators up to n ranked in order of magnitude - for example,

$$F_5 = \left\{ \frac{0}{1}, \frac{1}{5}, \frac{1}{4}, \frac{1}{3}, \frac{2}{5}, \frac{1}{2}, \frac{3}{5}, \frac{2}{3}, \frac{3}{4}, \frac{4}{5}, \frac{1}{1} \right\}. \text{ Each fraction is the mediant of its neighbours } \left(\frac{n_1 + n_2}{d_1 + d_2} \right).$$

For an adjacent pair $\frac{a}{b}, \frac{c}{d} : bc - ad = 1$. Because the sequence of fractions removes

degenerate common factors from the numerator and denominator, they are relatively prime and hence $|F_n| = |F_{n-1}| + \phi(n)$ the *totient* of positive integers less than or equal to n that are

relatively prime to n , since F_n contains F_{n-1} plus all fractions $\frac{p}{n} : p$ is coprime to n .

Two Farey sequence equivalents of RH state:

$$(i) \sum_{k=1}^{m_n} |d_{k,n}| = O(n^r), \text{ any } r > 1/2 \text{ and } (ii) \sum_{k=1}^{m_n} d_{k,n}^2 = O(n^r), \text{ any } r > -1$$

$$d_{k,n} = a_{k,n} - \frac{k}{m_n}, \text{ where } m_n \text{ is the length of the Farey sequence } \{a_{k,n}, k = 1, \dots, m_n\}$$

This is saying that the Farey fractions are as evenly distributed as they can be (to order $n^{1/2}$) given that they are by definition not evenly distributed, but determined by fractions with all (prime) common factors removed. The same consideration applies to the asymptotic distribution of the primes - they are as evenly distributed as they can be (to order $n^{1/2}$ from $\text{li}(n)$) - given that they are not evenly distributed, being those integers with no other factors.

(b) Number Fields: Dedekind zeta and Hecke L-functions

Let us now take a glance at number fields, which have their own zeta and L -functions, such as the Dedekind zeta and Hecke L -functions for the Gaussian integers.

The Gaussian integers $\mathbf{Z}[i]$, are defined by $x^2 + 1 = 0$, appending $\pm i$ to the integers, resulting in the lattice of complex numbers with integer real and imaginary parts. Here we have

$$\zeta_o = \sum_{0 \neq \alpha \in \mathcal{O} \bmod \mathcal{O}^\times} \frac{1}{(N\alpha)^z} = \frac{1}{4} \sum_{m,n \text{ not both } 0} \frac{1}{(m^2 + n^2)^z} = \prod_{\omega \text{ prime}} \frac{1}{1 - (N\omega)^{-z}}, \text{ where } N\alpha \text{ is the norm of the}$$

ideal $\mathbf{Z}[i] / \alpha \mathbf{Z}[i]$, which is uniquely expressible as an Euler product of prime ideals. This has a functional equation $\pi^{-z} \Gamma(z) \zeta_o(z) = \pi^{-(1-z)} \Gamma(1-z) \zeta_o(1-z)$, the Mellin transforms central in establishing this relationship (see appendix 2) act as a bridge which can define the function more accurately in the central region.

Correspondingly Hecke L -functions can be defined as follows. Consider the multiplicative group $\chi : \mathbf{Z}[i] \rightarrow S^1$, $\chi(\alpha) \rightarrow (\alpha / \bar{\alpha})^l$, $l \in \mathbf{Z}$. To give the same value on every generator this

requires l to be trivial on units, hence $1 = \chi(i) = \left(\frac{i}{-i} \right)^l = (-1)^l$, so $l \in 2\mathbf{Z}$. We then have for

each such l a Hecke L -function:

$$L(z, \chi) = \sum_{0 \neq \alpha \in \mathcal{O} \bmod \mathcal{O}^\times} \frac{\chi(\alpha)}{(N\alpha)^z} = \frac{1}{4} \sum_{m,n \text{ not both } 0} \frac{(\alpha / \bar{\alpha})^l}{(m^2 + n^2)^z} = \prod_{\omega \text{ prime}} \frac{1}{1 - \chi(\omega)(N\omega)^{-z}} \text{ where the primes are}$$

now those of Gaussian integers (a, b) , having units $\pm 1, \pm i$, with primes a unit times one of 3

types: $1+i$, a real prime which isn't a sum of squares ($p \bmod 4 = 3$), or has a^2+b^2 a prime ($p \bmod 4 = 1$). Again we have a functional equation:

$$\pi^{-(z+|l|)} \Gamma(z+|l|) L(z, \chi) = (-1)^l \pi^{-(1-z+|l|)} \Gamma(1-z+|l|) L(1-z, \chi)$$

The profiles of these functions with their analytic continuations are shown in fig 2, requiring, in addition to the functional equations, use of Mellin transform integral formulae in the critical strip:

$$\xi_o(z) = \pi^z \Gamma(z) \int_1^\infty (y^z + y^{1-z}) \frac{\theta(iy) - 1}{4y} dy, \quad \theta(iy) = \sum_{m,n \in \mathbb{Z}} e^{-\pi(m^2+n^2)y} = \left(\sum_{n \in \mathbb{Z}} e^{-\pi n^2 y} \right)^2$$

$$L(z, \chi) = \pi^{z+|l|} \Gamma(z+|l|) \int_1^\infty (y^z + (-1)^l y^{1-z}) \frac{\theta_\chi(iy)}{4y} dy, \quad \theta_\chi(iy) = \sum_{m,n \in \mathbb{Z}} (m \pm in)^{2|l|} y^l e^{-\pi(m^2+n^2)y}$$

Counting the coefficients of the Dirichlet sum over the sums of squares, we find:

$$\xi_0(z) = 1 + 2^{-z} + 0 + 4^{-z} + 2 \cdot 5^{-z} + 0 + 0 + 8^{-z} + \dots$$

In terms of our original primes in \mathbb{Z} , the Gaussian primes fall into three cases, shown in fig 2:

(i) $p \bmod 4 = 1$ **split**: $(m^2+n^2) = 4n+1$: $4n+k$ prime - two square roots of -1 (in the finite field F_{p^m} $m>1$) (ii) $p \bmod 4 = 3$ **inert**: $(0, \pm 4n+3)$ $(\pm 4n+3, 0)$ - no square root of -1 in F_{p^m} , m odd but 2 if m even; (iii) $p = 2$ **ramified**: $(\pm 1 \pm i)$ - one square root of -1.

When we go back to Dedekind zeta's Euler product, we see that the product over Gaussian primes coincides exactly with an Euler product over integer primes incorporating the above cases and both generate the sum coefficients from unique natural prime power factorisations:

$$\prod_{\omega \text{ prime}} \frac{1}{1 - (N\omega)^{-z}} = \left(\frac{1}{1 - (1^2 + 1^2)^{-z}} \right) \left(\frac{1}{1 - (3^2)^{-z}} \right) \left(\frac{1}{1 - (1^2 + 2^2)^{-z}} \right) \left(\frac{1}{1 - (2^2 + 1^2)^{-z}} \right) \dots$$

$$= \frac{1}{1 - (2)^{-z}} \prod_{p \bmod 4 = 1} \frac{1}{(1 - (p)^{-z})^2} \prod_{p \bmod 4 = 3} \frac{1}{1 - (p)^{-2z}} = \left(\frac{1}{1 - (2)^{-z}} \right) \left(\frac{1}{1 - (3)^{-2z}} \right) \left(\frac{1}{(1 - (5)^{-z})^2} \right) \dots$$

$$= 1 + 2^{-z} + 0 + 4^{-z} + 2 \cdot 5^{-z} + 0 + 0 + 8^{-z} + \dots$$

(c) Elliptic Curves

The Hasse-Weil L -function of an elliptic curve E is generated by taking the function $E(Q)$ over Q , or a field extension F , and estimating the number of rational points (Silverman 1986). Factoring mod p , for primes p , to get a set of A_p points on the curve $E(F_p)$ in the finite prime field F_p , giving up to a maximum of $p+1$ points in F_p (including the point at infinity). We then let $a_p = p+1-A_p$ the number of missing points. For example, for the elliptic curve $y^2 + y = x^3 - 7x + 6$, $(0,2)$, $(1,0)$, $(1,4)$, $(2,0)$, $(2,4)$, $(3,1)$, $(3,3)$, $(4,1)$, $(4,3)$, (∞, ∞) are solutions mod 5, giving $a_5 = 5+1-10 = -4$. The process is now more complicated but ultimately is a type of non-mode-locked distribution rule among the natural primes, via the Euler product.

$$L(E, z) = \sum_{n=1}^{\infty} a_n n^{-z} = \prod_p L_p(E, z), \quad L_p(E, z) = \begin{cases} (1 - a_p p^{-z} + p^{1-2z})^{-1} & \text{good reduction} \\ (1 - a_p p^{-z})^{-1} & \text{bad reduction} \end{cases}$$

where bad reduction i.e. a singularity of $E(F_p)$ results from repeated roots in F_p , when $a_p = \pm 1$, depending on the splitting or inertness of p for multiplicative reduction ($p|N$ but not p^2) of E , or is 0 if $p^2|N$ (additive reduction), where N is the conductor, the 'effective' product of bad primes (see below). Setting $L^*(E, z) = N^{z/2} (2\pi)^{-z} \Gamma(z) L(E, z)$, we have the functional

equation $L^*(E, z) = \varepsilon L^*(E, 2 - z)$, where $\varepsilon = \pm 1$. In this case the L -function has weight 2 and thus has steadily increasing Dirichlet coefficients, so its critical line is moved to the right to 1, with the a_n generated from the Euler product, which is convergent for $x > 3/2$. Once again, it is the product on the RHS defining the process, through an arithmetic process involving the natural primes, with the Dirichlet series merely being formed as a reflection of this rule.

The conductor, as the 'effective' product, differs from the discriminant - a product of all bad prime factors. It consists of factors 1 for good reduction, p for multiplicative reduction, and p^2 for additive, except in the cases 2, 3 where the exponent may have an additional 'wild' component, increasing it up to 5 for 2 and 3 for 3, depending on the number of irreducible components (without multiplicity) of the 'special Neron fibre' using Tate's algorithm (Tate, Silverman 1994, Cremona 1997).

A good example is the elliptic curve $y^2 = x^3 - 11x^2 + 385$ (Lozano-Robledo), with additive reduction on 2, 11, split multiplicative on 5 and inert multiplicative on 7 and 461:

$$L(z) = (1 - 5^{-z})^{-1} (1 + 7^{-z})^{-1} (1 + 461^{-z})^{-1} \prod_{p \neq 2, 5, 7, 11, 461} (1 - a_p p^{-z} + p^{1-2z})^{-1} = 1 - \frac{2}{3^z} + \frac{1}{5^z} - \frac{1}{7^z} + \dots,$$

with conductor $N = 2^3 \cdot 11^2 \cdot 5 \cdot 7 \cdot 461 = 15618680$ and root number -1.

Elliptic curves have a group multiplication connecting any two points on the curve to the third point of intersection of the line through them, as illustrated in fig 2. The Birch and Swinnerton-Dyer conjecture asserts that the rank of the Abelian group $E(F)$ of points of E is the order of the zero of $L(E, z)$ at $z = 1$. Even rank gives $\varepsilon = 1$ and odd $\varepsilon = -1$ in the functional equation above. The group may also have finite torsion elements.

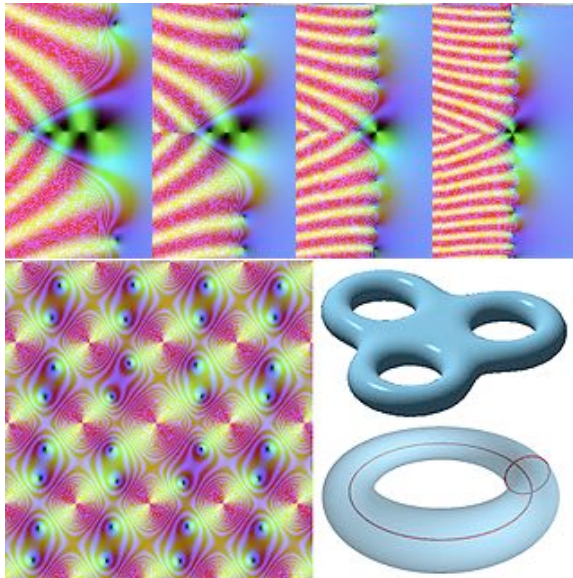


Fig 3: Above: Elliptic curves 11a, 37a, 389a, and 5077a with coefficients $[0, -1, 1, -10, -20]$, $[0, 0, 1, -1, 0]$, $[0, 1, 1, -2, 0]$ and $[0, 0, 1, -7, 6]$ illustrating the cases 0 (no zero at 1), 1, 2 and 3 of the Birch and Swinnerton-Dyer conjecture in the multiple-ray angular variation of the argument of the L -function round the central point. Lower left: Weierstrass function and lower right the genus. The doubly periodic nature of the function and a one and three-holed torus (see modular forms) are illustrated below left, with the two periodicities illustrated on the one torus.

If one takes the defining equation of an elliptic curve, one can generate an algebraic function, which is single-valued on a surface, enabling the elliptic curve to also be represented as a mapping on a torus. This parametrization, via the Weierstrass function defines a "fundamental

parallelogram" in the complex plane, representing the two periodicities. Elliptic functions over C are thus genus-1 curves, topologically equivalent to embeddings of a torus in $PC \times PC$ where PC is the complex projective plane or Riemann sphere derived by adding a single point at ∞ to C . Higher degree curves generate higher genus examples.

(d) Modular and Automorphic Forms

Complementing the L -functions of elliptic curves are those of modular forms. The toroidal nature of the elliptic function, causes it to be periodic on a parallelogram in C , resulting in a

deep relationship with another kind of L -function. A modular function is a meromorphic function (analytic with poles) in the upper half-plane H , which is conserved by the modular group $SL(2, \mathbb{Z})$ of integer 2×2 matrices of determinant 1 i.e. $f(az+b)/(cz+d) = f(z)$. More generally we have modular of weight w (necessarily even) if $f(az+b)/(cz+d) = (cz+d)^w f(z)$. If it is holomorphic (fully analytic) in the upper half-plane (and at ∞) we say it is a *modular form*. If it is zero at ∞ we say it is a *cusp form*. We can also consider modular forms over congruence subgroups of $SL(2, \mathbb{Z})$ such as $\Gamma_0(N)$ by factoring mod N . These are defined in detail in the next section on the Selberg zeta function. Since $M \setminus N \Rightarrow \Gamma_j(N) \subset \Gamma_j(M)$ a form in $\Gamma_j(M)$ is also in $\Gamma_j(N)$. While there are only a small number of elliptic curve L -functions for a given N there can be hundreds or even thousands of modular forms for a given N .

Since $f(z+1) = f(z)$, f is periodic, so we can express it as a Fourier series in z or a Laurent series

in q $f(z) = \sum_{n=-\infty}^{\infty} a_n e^{2\pi i n z} = \sum_{n=-\infty}^{\infty} a_n q^n$. If f has only simple isolated pole singularities we have only a finite number of negative powers of q and if f is analytic, we have a Taylor expansion

$$f(z) = \sum_{n=0}^{\infty} a_n e^{2\pi i n z} = \sum_{n=0}^{\infty} a_n q^n, \quad q = e^{2\pi i z}. \text{ Using the Mellin transform } M(f, z) = \int_0^{\infty} f(t) t^{z-1} dt, \text{ we can}$$

derive the L -function $L(f, z) = (2\pi)^2 M(f, z) / \Gamma(z) = \sum_{n=1}^{\infty} a_n n^{-z}$, which again has a functional

equation. If $L^*(f, z) = N^{z/2} (2\pi)^{-z} \Gamma(z) L(f, z)$, then $L^*(f, z) = (-1)^{w/2} L^*(f, w - z)$, and L^* is meromorphic on \mathbb{C} . For a complete derivation, see appendix 2.

In the case of weight $w = 2$ there is thus a correspondence between the functional equations of elliptic curves and modular forms. The Taniyama-Shimura modularity theorem asserts that every elliptic curve over \mathbb{Q} has a modular form parametrization based on the conductor, essentially through the periodicities induced by its toroidal embedding, a relationship pivotal in the proof of Fermat's last theorem (Daney), where Andrew Wiles (1995) showed that any semi-stable elliptic curve (one having only multiplicative bad reductions) is modular. But if we can find $x^n + y^n = z^n$ then the elliptic curve $Y^2 = X(X - x^n)(X + y^n)$ is semi-stable but not modular. Hence the proof!

This is an example where a classical unsolved mathematical problem has been resolved by appealing to the conceptual sensitivity of advanced forms of abstract mathematics. Many people hope that RH may succumb to a similar strategy, but this remains unclear, because the distribution of the natural primes lies right at the heart of our concept of number and the relationship between counting, leading to addition; and replication, leading to multiplication.

Modular forms that are eigenfunctions of all Hecke operators $T_n f = \lambda_n f = a_n f$, where

$$T_n f(z) = n^{k-1} \sum_{M \in \Gamma \backslash M_n} (cz+d)^{-k} f\left(\frac{az+b}{cz+d}\right), \quad M_n = \left\{ A = \begin{pmatrix} a & b \\ c & d \end{pmatrix} : |A| = n \right\}, \text{ have the equivalent Euler product } L(f, z) = \prod_{p|N} (1 - a_p p^{-z})^{-1} \prod_{p \nmid N} (1 - a_p p^{-z} + p^{2k-1-2z})^{-1} \text{ (Cogdell, Lozano-Robledo).}$$

Conveniently each eigenfunction satisfies all the Hecke operators T_n simultaneously.

One can calculate Hecke operators and matrices in terms of the power series $f(q) = \sum_m a_m q^m$:

$T_p(f(q)) = \sum_{m \in \mathbb{Z}} (b_m q^m = \sum_{m \in \mathbb{Z}} (a_{mp} + p^{k-1} a_{m/p}) q^m, a_{m/p} = 0, m/p \notin \mathbb{Z}, p \text{ prime, which is generally sufficient for determining eigenvalues and eigenforms.}$

For example for $N=43$, we have echelon basis: $f = q + 2*q^5 - 2*q^6 - 2*q^7 - q^9 + O(q^{10})$, $g = q^2 - 1/2*q^4 + q^5 - 3/2*q^6 - q^8 - 1/2*q^9 + O(q^{10})$, $h = q^3 - 1/2*q^4 + 2*q^5 - 3/2*q^6 - q^7 + q^8 - 1/2*q^9 + O(q^{10})$ Applying the above formula for T_2 to f , we have $b_1 = a_2 + 2.0 = 0$, $b_2 = a_4 + 2.0 = 2$,

$b_3 = a_6 + 2.0 = -2$, giving the first row of the Hecke matrix $T_2 = \begin{bmatrix} 0 & 2 & -2 \\ 1 & -1/2 & -3/2 \\ 0 & -1/2 & -3/2 \end{bmatrix}$, which has

eigenvalues $a_0 = -2$ and $a_1 = \pm\sqrt{2}$. These eigenvalues give normalized eigenvectors $v = q - 2*q^2 - 2*q^3 + 2*q^4 - 4*q^5 + 4*q^6 + q^9 + O(q^{10})$, $w_{a1} = q + a_1*q^2 - a_1*q^3 + (2-a_1)*q^5 - 2*q^6 + (a_1 - 2)*q^7 - 2*a_1*q^8 - q^9 + O(q^{10})$, which are *newforms*, normalized eigenforms of level N not arising from an $M < N$, defined as a linear combination of the above echelon basis functions, the first of which is the elliptic curve $e43a$. One can confirm they are eigenvectors using the same formula, e.g. $T_2(v) = -2v$. By inverting the resulting basis transformation matrix

$A = \begin{bmatrix} 1 & -2 & -2 \\ 1 & \sqrt{2} & -\sqrt{2} \\ 1 & -\sqrt{2} & \sqrt{2} \end{bmatrix}$, we can in turn express the echelon basis in terms of the eigenforms.

Each elliptic function with conductor N is thus associated with a *newform* - (Stein).

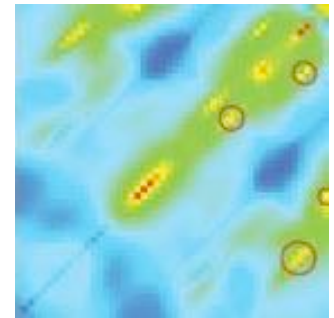
(e) Maass forms

These are modular differential eigenfunctions of the hyperbolic Laplace wave function, discussed further in the next section, which commute with $SL(2, \mathbb{Z})$, and generate a vast spectrum of eigenforms, having complex gamma factors $\lambda_i = e \pm ir$, $i = 1, 2$, where $e=0,1$ and $\varepsilon = 1, -1$ for even and odd functions, where the eigenvalue is $1/4 + r^2$, and a slightly more

complicated Fourier series $f(z) = \sqrt{y} \sum_{n=1}^{\infty} a_n K_{ir}(2\pi |n| y) e^{2\pi i x}$, with K_{ir} the modified Bessel

function. For $N=11$ there are around 1000 such forms over Γ_0 (Booker et. al. 2006, Farmer and Lemurell), which can be located by searching for eigenvalue hot spots.

Fig 4: Hot regions in $(u,v)=[10, 20]^2$ (red) with 4 non-trivial degree 3 examples not simply a product of lower dimensional examples circled (18.902, 11.761), (16.741, 16.232), (20.021, 14.070), (19.179, 17.702) and quasi-trivial examples on the diagonal $u = v$ at 13.779, 17.738, 19.423 (Bian)



Two degree 3 L -functions are illustrated in fig 2 (Bian 2010, Booker 2008), based on $GL(3)$ Maass forms, which are written in terms of a three dimensional generalized upper half-plane $w=XY$, where

$$X = \begin{pmatrix} 1 & x_2 & x_3 \\ 0 & 1 & x_1 \\ 0 & 0 & 1 \end{pmatrix}, Y = \begin{pmatrix} y_1 y_2 & 0 & 0 \\ 0 & y_1 & 0 \\ 0 & 0 & 1 \end{pmatrix}, x_i, y_i \in \mathbb{R}, y_i > 0. \text{ The form}$$

$\varphi(w)$ is an eigenfunction of the Laplacian, which is preserved under $SL(3, \mathbb{Z})$. This has an extended Fourier series, which can be used to define a complex L -function with a degree 3 Euler product

$$L(z, \varphi \times \chi) = \prod_{p \text{ prime}} \left(1 - A(1, p) \chi(p) p^{-z} + A(p, 1) \chi^2(p) p^{-2z} - \chi^3(p) p^{-3z} \right)^{-1}$$

where $\chi(p)$ is a Dirichlet character 'twisting' the L -function and $A(p, q)$ are Fourier coefficients of the Maass cusp form with eigenvalues (λ_1, λ_2) , $\text{real}(\lambda_i) = 1/3$.

These also obey a functional equation of the form $\Lambda(z, \varphi \times \chi) = \varepsilon_\chi^3 \Lambda(1 - z, \tilde{\varphi} \times \bar{\chi})$, where \sim takes coefficients and gamma factors to their conjugates, and

$$\Lambda(z, \varphi \times \chi) = N^{z/2} \pi^{-(z-\alpha)/2} \Gamma\left(\frac{z-\alpha}{2}\right) \pi^{-(z-\beta)/2} \Gamma\left(\frac{z-\beta}{2}\right) \pi^{-(z-\gamma)/2} \Gamma\left(\frac{z-\gamma}{2}\right) L(z, \varphi \times \chi).$$

Continuing this process to even higher degrees, Farmer, Ryan and Schmidt (2010) have constructed functional equations for L -functions of degrees 4, 5, 10, 14, and 16, using holomorphic Siegel modular forms on $\text{Sp}(4, \mathbb{Z})$ and tested the functional equation at sample points of an L -function of degree 10.

Each of the types of L -function discussed has an Euler product in which the natural primes determine the Dirichlet series coefficients and admit a functional equation determined by the Dirichlet series, a finite number of gamma parameters, determined by the underlying topology generating the Euler product, the conductor, and a sign factor (Dokchitser, Harron):

$$L^*(f, z) = N^{z/2} (2\pi)^{-z} \Gamma\left(\frac{z+\lambda_1}{2}\right) \cdots \Gamma\left(\frac{z+\lambda_d}{2}\right) L(f, z), \text{ then } L^*(f, z) = \varepsilon L^*(f, w - z)$$

where $|\varepsilon| = 1$, $\varepsilon = e^{2\pi i k/n}$ for Dirichlet L -functions $\varepsilon = \pm 1$ otherwise. The gamma factors can be used to define a generalized Mellin transform technique for describing L -functions in the critical strip for moderate y values (Dokchitser). These types can be generalized in motivic L -functions (Deligne, Dokchitser).

The upshot of this study of a reasonable spread of exotic zeta and L -functions, is that their non-trivial zeros lie on the weighted critical line if and only if they are generated by an underlying natural primal distribution through an Euler product with an analytic continuation, meaning that all these functions are singing the same unproven song about the one natural prime distribution and its non-mode-locked character. This suggests widening the investigation to consider more general classes of Euler products based on other distributions than that of the natural primes.

Into the Looking Glass World: Selberg and Dynamical zeta Functions

To understand the other side of the coin from trying to find out why the natural prime-based zeta and L -functions have their zeros on the critical line, we turn to dynamical zeta functions, based on the lengths of orbits, rather than through elaborate algebraic transformations of the natural primes. As critical examples of these can be proved to obey the Riemann hypothesis, they provide an exotic alternative reality, giving critical insights into why the zeros fall on the critical line with dynamical systems.

(a) Graphical and Diffeomorphism Zeta Functions

Consider a directed graph with vertices (v_1, \dots, v_n) connected by directed edges $e_m = \langle v, v' \rangle \in E$.

For any prime (not a multiple of a shorter path) closed path τ of length $|\tau|$, we define the zeta

function $\zeta(z) = \prod_{\tau} (1 - z^{|\tau|})^{-1}$. It can also be easily shown that $\zeta(z) = \exp\left(\sum_{n=1}^{\infty} \frac{z^n}{n} N(n)\right)$, where $N(n)$ is the number of vertex strings representing all paths in the graph of length n (Pollicott 2013).

It turns out that it is straightforward to represent $\zeta(z)$ in terms of the eigenvalues λ_i of its transition

matrix $A : a_{v,v'} = \begin{cases} 1, \langle v, v' \rangle \in E \\ 0, \langle v, v' \rangle \notin E \end{cases}$. Since $N(n) = \text{trace}(A^n) / n = \sum_i \lambda_i^n / n$ we can apply the second

formula above to get $\zeta(z) = \det(I - zA)^{-1}$, assuming A is aperiodic, leading to a zeta function, which is the reciprocal of a polynomial, as shown in the example in the figure.

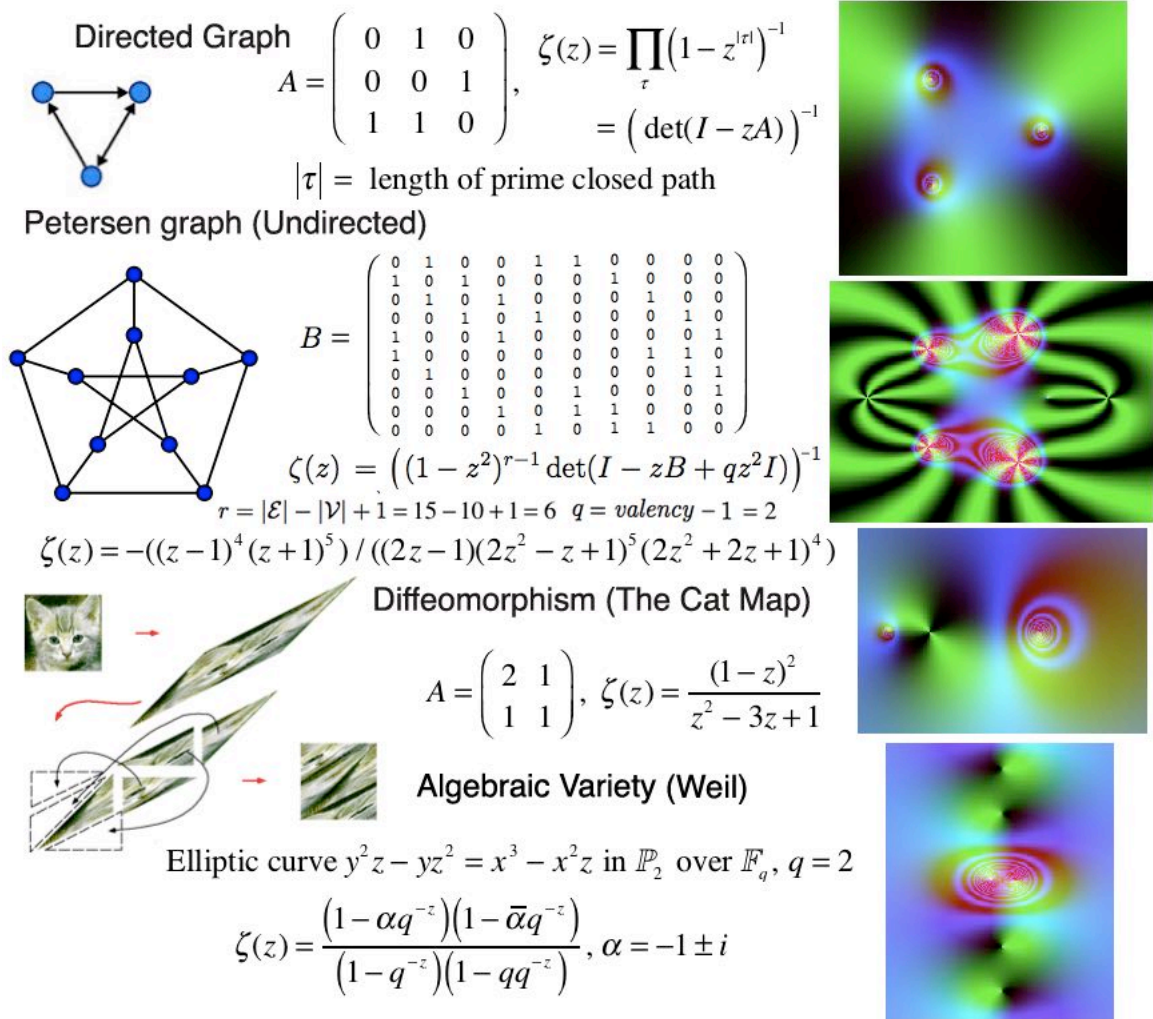


Fig 5: Examples of zeta functions of graphs and diffeomorphisms

We can apply the same analysis to undirected graphs, such as the Petersen graph illustrated, to derive a similar zeta function, as a rational function, depending on the valency and vertex and edge count. A further concept that will become key is to consider the Laplacian – the linear operator

$\Delta : l^2(v) \rightarrow l^2(v)$ on functions $w \in l^2(v)$ on the vertices, defined by

$\Delta(w(v)) = w(v) - \frac{1}{q+1} \sum_{\langle v, v' \rangle \in E} w(v')$. This can be represented as the matrix $I - \frac{1}{q+1} B$, and is self-

adjoint having eigenvalue spectrum in $[-1, 1]$.

One can extend these ideas to diffeomorphisms. Let $f : M \rightarrow M$ be a C^∞ diffeomorphism of a compact manifold and denote $\text{Fix}(f^n) = \{x : f^n(x) = x\}$, then we can define

$\zeta(z) = \exp\left(\sum_{n=1}^{\infty} \frac{z^n}{n} \text{Fix}(f^n)\right)$. The number $N(n)$ of periodic points grows exponentially i.e. the topological entropy $h(f) = \lim_{n \rightarrow +\infty} \log(N(n)) / n > 0$. Like the previous examples, the zeta function can be extended to a meromorphic function on the complex plane, which is again a rational quotient of polynomials.

For example the Arnol'd Cat map $f : T^2 \rightarrow T^2$ a toroidal automorphism associated to

$A = \begin{pmatrix} 2 & 1 \\ 1 & 1 \end{pmatrix} \in SL(2, \mathbb{Z})$ has $\zeta(z) = \frac{(1-z)^2}{z^2 - 3z + 1}$. This is famous for chaotic Poincare recurrence,

where a single dense orbit will bring the initial 'cat' image back arbitrarily close to the starting position over exponentiating time intervals.

Also included for completeness a Weil zeta function example (Oort 2014). These obey the RH, although this goes no way to proving the hypothesis for Riemann's zeta (see **appendix 3**).

(b) Hyperbolic Space, Orbifolds and Discrete Subgroups of $SL(2, \mathbb{R})$

Hyperbolic and elliptic geometry extends Euclidean geometry to surfaces of positive and negative curvature by amending the parallel postulate so that parallel geodesics either never meet (hyperbolic) or meet more than once (elliptic). There are two favourite models for the hyperbolic plane, the Poincare disc $D = \{z \in \mathbb{C} : |z| < 1\}$ and the half-plane $H = \{z \in \mathbb{C} : \text{Im}(z) > 0\}$ with

hyperbolic metrics $d_D(z, z') = 1 + \frac{2|z - z'|^2}{(1 - |z|^2)(1 - |z'|^2)^2}$ and $d_H(z, z') = 1 + \frac{2|z - z'|^2}{2yy'}$, $z = x + iy$. These

in turn lead to differential lengths and volumes in which the Laplacian differentiation operator

$\Delta : L^2(V) \rightarrow L^2(V)$ takes the forms $\Delta_D = \frac{1}{4}(1 - |z|^2)^2 \left(\frac{\partial^2}{\partial x^2} + \frac{\partial^2}{\partial y^2} \right)$ and $\Delta_H = y^2 \left(\frac{\partial^2}{\partial x^2} + \frac{\partial^2}{\partial y^2} \right)$.

The Laplace eigenfunctions – called Maass wave forms – are analytic functions u from the half-plane to \mathbb{C} which are automorphic ($u(\gamma z) = \gamma u(z)$), integrable and an eigenfunction of $\Delta : \Delta u + \lambda u = 0$, $\lambda > 0$.

In the half-plane model, hyperbolic isometries $g : H \rightarrow H$ act by fractional linear, or Mobius

transformations $g(z) = \frac{az + b}{cz + d} : A = \begin{pmatrix} a & b \\ c & d \end{pmatrix} \in PSL(2, \mathbb{R}) = SL(2, \mathbb{R}) / \{\pm 1\}$ the subgroup of

$SL(2, \mathbb{R})$ the group of real 2×2 matrices with determinant 1, by identifying 1 and -1 since A and $-A$ result in the same g . We say that g , or its fixed point(s), are *elliptic*, *hyperbolic* or *parabolic* depending on whether $|\text{trace}(g)| = |a + d| < 2$, $= 2$, or > 2 . A parabolic fixed point is degenerate, lies in the boundary of the half-plane and is called a cusp. Elliptic points lie in pairs, one in each half-plane. Hyperbolic points x , and its 'conjugate' x^* , appear in pairs on the boundary. A geodesic γ is either a half-circle orthogonal to the real line or a vertical line.

Each element of $SL(2, \mathbb{R})$ has a unique factorization NAK , where

$$A = \begin{pmatrix} 1 & b \\ 0 & 1 \end{pmatrix}, N = \begin{pmatrix} a & 0 \\ 0 & 1/a \end{pmatrix}, K = \begin{pmatrix} \cos(\theta/2) & \sin(\theta/2) \\ -\sin(\theta/2) & \cos(\theta/2) \end{pmatrix}, a, b \in \mathbb{R}, a > 0, \theta \in [0, 2\pi)$$

Hyperbolic spaces can also be generated by the action of a discrete subgroup Γ of $PSL(2, \mathbb{R})$ to form quotient spaces $M = \Gamma \backslash H$, which can take the form of orbifolds – equivalents of topological manifolds but locally modeled using quotients of open subsets of \mathbb{R}^n by finite group actions rather than on the usual manifold open subsets of \mathbb{R}^n .

If $\pi: H \rightarrow M$, $\pi(z) = \Gamma z$, then $\gamma^* = \pi(\gamma)$ is a closed geodesic on M iff each $\gamma \in \pi^{-1}(\gamma^*)$ has end points which are conjugate hyperbolic fixed points. This gives a 1-1 correspondence between hyperbolic conjugacy classes $\{[P] = APA^{-1} : A, P \in \Gamma, \text{trace}(P) > 2\}$. Any such P can be written as the positive power of a primitive element $P = P_0^n$, so every geodesic has a minimal length.

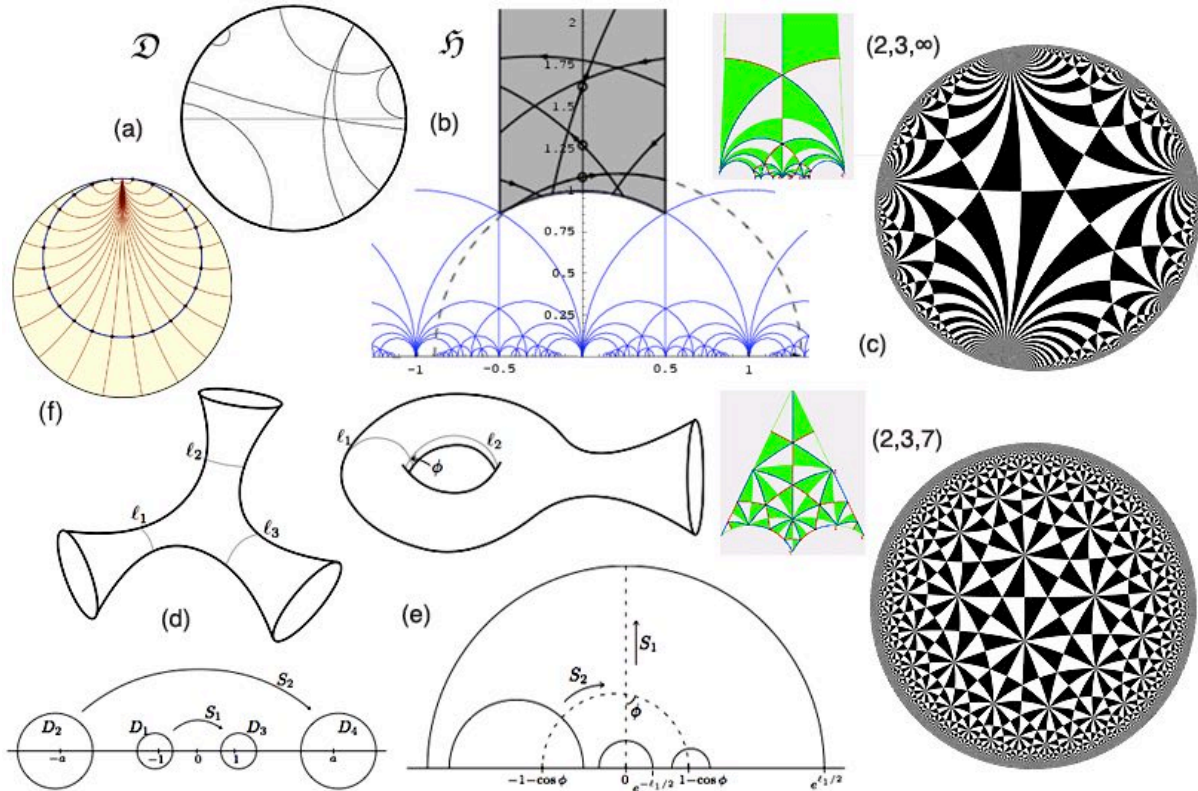


Fig 6: (a) The Poincaré disc model showing geodesics. (b) A fundamental domain for the modular group forming a tessellation of the half-plane model with a geodesic flow inset. (c) Modular group (2,3,∞) and triangle group (2,3,7) checker-boards on both models. (d) The tri-funnel and (e) the funnel torus with Mobius maps illustrated. Unlike elliptic and Euclidean non-compact spaces, which are restricted to spheres, Euclidean space and a few flat tori, hyperbolic non-compact spaces have diverse structures. (f) A horocycle – a curve whose perpendicular geodesics all converge asymptotically in the same direction.

The modular group $\Gamma = SL(2, \mathbb{Z})$, with the same projective identification of ± 1 , as above consists of all determinant 1 matrices with integer coefficients. This forms a discrete subgroup of $PSL(2, \mathbb{R})$, which forms a tessellation of H by hyperbolic triangles when a

fundamental domain such as $D = \{z \in H : |z| > 1, |\operatorname{Re}(z)| < 1/2\}$ is transformed by applying each of the elements of the modular group. Such tessellations can be subdivided into chequer-board arrangements by partitioning the fundamental domain as shown in fig 6.

One can likewise form congruence subgroups $\Gamma(n)$ of Γ by taking the kernel of the homomorphism reducing the elements of $\Gamma \bmod n$:

$$\Gamma(N) := \left\{ \begin{pmatrix} a & b \\ c & d \end{pmatrix} \in \Gamma : \begin{pmatrix} a & b \\ c & d \end{pmatrix} \equiv \begin{pmatrix} 1 & 0 \\ 0 & 1 \end{pmatrix} \bmod N \right\}$$

$\Gamma(n)$ is in turn a subgroup of $\Gamma_0(n)$, the Hecke congruence group of matrices with $c = 0 \bmod n$. There are also larger groups such as $GL(2, \mathbb{Z})$, which includes matrices of determinant -1 acting on the conjugate of z . One can form quotients by a variety of other Fuchsian groups (discrete subgroups of $PSL(2, \mathbb{R})$), including triangle groups, which form group variants of $SL(2, \mathbb{Z})$, where the point at infinity is moved to a finite position. One can also form a variety of hyperbolic orbifolds by factoring by Schottky groups, where a set of Mobius transformations on disjoint circles, mapping the inside of one to the outside of another, are used to generate spaces such as the tri-funnel and funnel torus. For an integer $q \geq 3$ the Hecke triangle group $G(n)$ is generated by the maps $S : z \rightarrow 1/z$, $T : z \rightarrow z + \lambda_q$,

$\lambda_q = \cos(\pi/q)$ with fundamental domain $D = \{z : |\operatorname{Re}(z)| \leq \lambda/2, |z| > 1\}$. In a similar way we can generate Mobius maps for quotient spaces such as the tri-funnel and funnel torus, using the maps defined as follows:

Tri-funnel	Funnel torus
$S_1 := \begin{pmatrix} \cosh(\ell_1/2) & \sinh(\ell_1/2) \\ \sinh(\ell_1/2) & \cosh(\ell_1/2) \end{pmatrix},$	$S_1 = \begin{pmatrix} e^{\ell_1/2} & 0 \\ 0 & e^{-\ell_1/2} \end{pmatrix},$
$S_2 := \begin{pmatrix} \cosh(\ell_2/2) & a \sinh(\ell_2/2) \\ a^{-1} \sinh(\ell_2/2) & \cosh(\ell_2/2) \end{pmatrix},$	$S_2 = \begin{pmatrix} \cosh(\ell_2/2) - \cos \phi \sinh(\ell_2/2) & \sin^2 \phi \sinh(\ell_2/2) \\ \sinh(\ell_2/2) & \cosh(\ell_2/2) + \cos \phi \sinh(\ell_2/2) \end{pmatrix}.$
with $a > 0$ solving $\operatorname{tr}(S_1 S_2^{-1}) = 2(\cosh \ell_3/2)$.	

(c) Selberg Zeta Functions

We now come to the Selberg zeta function for closed geodesics on the compact hyperbolic surface V and to Selberg's trace formula, which is key to many of the results, including RH for Selberg zetas. Riemann's original work relating the prime distribution to the zeros of the Riemann zeta function depended on taking Fourier transforms.

The von Mangoldt prime counting formula

$$\psi(x) = \sum_{n \leq x} \Lambda(n) = x - \sum_p \frac{x^\rho}{\rho} - \frac{1}{2} \ln(1 - x^{-2}) - \ln(2\pi) \quad \Lambda(x) = \begin{cases} \log p, & x = p^k \\ 0, & x \neq p^k \end{cases} \quad \text{is in effect an example}$$

of the Poisson summation formula $\sum_{m \in \mathbb{Z}} h(m) = \sum_{n \in \mathbb{Z}} \int_{\mathbb{R}} h(\rho) e^{2\pi i n \rho} d\rho$, in which the sum of values of a function is equal to the sum of its Fourier transforms, with the sum over logs of prime powers being equated to a sum over zeta zeros.

To illustrate the Poisson formula as a trace formula, we take as an example space the circle S^1 of length 2π (Marklof 2008). The positive Laplacian $-\Delta = -\frac{d^2}{dx^2}$, has eigenvalues $\lambda_m = m^2$, $m \in \mathbb{Z}$ satisfying $\Delta \varphi_m + \lambda_m \varphi_m = 0$, with eigenfunctions $\varphi_m(x) = (2\pi)^{-1/2} e^{imx}$.

Consider the linear operator $[Lf](x) = \int_0^{2\pi} k(x,y)f(y)dy$, with $k(x,y) = \sum_{m \in \mathbb{Z}} h(m)\varphi_m(x)\bar{\varphi}_m(y)$ with $L\varphi_m = h(m)\varphi_m$. Then $\text{trace } L = \sum_{m \in \mathbb{Z}} h(m) = \sum_{n \in \mathbb{Z}} h(\rho)e^{2\pi i n \rho} d\rho$.

The LHS consists of the eigenvalues of L while the RHS is a sum over periodic orbits of the geodesic flow on S^1 whose lengths are $2\pi|n|$, $n \in \mathbb{Z}$.

In the case of a compact Riemannian surface defined as the quotient of the hyperbolic plane by a discrete subgroups of $PSL(2, \mathbb{R})$, we have Laplacian $\left(\Delta + \kappa_n^2 + \frac{1}{4}\right)\psi = 0$ and can take two arbitrary functions $h(k)$, $g(l)$, which are Fourier transforms of one another

$h(\kappa) = \int_{-\infty}^{\infty} e^{i\kappa\lambda} g(\lambda) d\lambda$, $g(\lambda) = \int_{-\infty}^{\infty} e^{-i\kappa\lambda} h(\kappa) d\kappa$ and arrive at Selberg's trace formula

$$\sum_{j=0}^{\infty} h(\kappa_j) = \frac{\mu(D)}{4\pi} \int_{-\infty}^{\infty} v h(v) \tanh(\pi v) dv + \sum_p l_p \sum_{n=1}^{\infty} \frac{g(n l_p)}{2 \sinh(n l_p / 2)},$$

where $\mu(D)$ is the area of the fundamental domain. On the left is effectively a sum over eigenvalues $E_n = \frac{1}{4} + \kappa_n^2$, and on the right a sum over lengths l_p of the prime geodesics.

We will examine Selberg zeta functions in the context of a discrete subgroup Γ of $SL(2, \mathbb{R})$ and consider both the geodesic length spectrum $0 \leq l_1 \leq l_2 \leq \dots$ and the eigenvalue spectrum $0 \leq \lambda_1 \leq \lambda_2 \leq \dots$ of the hyperbolic Laplace operator Δ .

Selberg's zeta function is defined by $Z(s) = \prod_{\gamma} \prod_{n=0}^{\infty} (1 - e^{-(s+n)l(\gamma)})$, $\text{Re}(s) > 0$ where $l(\gamma)$ is the length of each primitive closed geodesic γ . As with the graph zeta functions, we can write

$Z(s) = \prod_{\gamma} \prod_{n=0}^{\infty} (1 - N(\gamma)^{-s-n})$, where $N(\gamma)$ is the solution of $\text{trace}(P) = N^{1/2} + N^{-1/2}$, $1 < N < \infty$, or

ε^2 for γ conjugate to $\pm \begin{pmatrix} \varepsilon & 0 \\ 0 & 1/\varepsilon \end{pmatrix}$, $\varepsilon > 1$,

Alternatively, we have the associated $\zeta(s) = \prod_{\gamma} (1 - e^{-sl(\gamma)})^{-1}$ having close comparisons in

definition with the Euler product definition of Riemann zeta $\zeta(s) = \prod_{p \text{ prime}} (1 - p^{-s})^{-1}$.

With relations $\zeta(s) = Z(s+1)/Z(s)$, $Z(s) = \prod_{n=0}^{\infty} \zeta(s+n)^{-1}$.

These ideas are theoretically encapsulated in the notion of the arithmetic zeta function defined as a product $\zeta(s) = \prod_x (1 - N(x)^{-s})^{-1}$ over the cardinalities $N(x)$ of 'closed' points whose residue field is finite, of a 'scheme' consisting of a topological space with the ring spectra over its open sets.

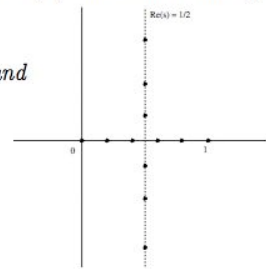
The number of geodesics: $\text{Card}\{\gamma : l(\gamma) < T\} \sim \frac{e^T}{T}, T \rightarrow \infty$ gives the prime number theorem for

Selberg zeta functions, just as the number of natural primes is asymptotic to $\frac{x}{\log x}$.

Because $Z(s)$ can be expressed as a product over eigenvalues, it has a meromorphic (infinitely differentiable except at isolated poles) continuation over \mathbb{C} and has zeros at the spectral parameters defined by $s_j : s_j(1 - s_j) = \lambda_j$, where λ_j is an eigenvalue of Δ and because the Laplacian is self-adjoint, the eigenvalues are all real and so the zeros are all on the critical line $x = 1/2$. We thus arrive at the result that the Riemann hypothesis is true for the Selberg zeta function:

Theorem (Selberg). *The zeros of the Selberg zeta function $Z(s)$ can be described by:*

1. $s = 1$ is a simple zero;
2. $s_n = \frac{1}{2} \pm i\sqrt{\frac{1}{4} - \lambda_n}$, for $n \geq 1$, are "spectral zeros"; and
3. $s = -m$, for $m = 0, 1, 2, \dots$, are "trivial zeros".



The picture of the zeros is actually more complicated than indicated in the above theorem of Selberg. The eigenvalue spectrum generally falls into two parts. A discrete spectrum where $\lambda > 1/4$ where the spectral parameter $s = 1/2 \pm ri$, $r \in \mathbb{R}$, giving non-trivial zeros on the critical line $x = 1/2$. The discrete spectrum is embedded in a continuous spectrum, in which the eigenvalues $\lambda \leq 1/4$ $s \in [0, 1]$ related to the residues of poles of the Eisenstein series analytically continued to cusp forms. Other zeros for complex values with $\text{Re}(z) < 1/2$ are related to the resonances of the scattering matrix and there are also trivial zeros and poles at negative integers and others at half-integer points.

However these results depend essentially on the trace formula and, although the asymptotics of the set of eigenvalues are understood, and we know the non-trivial zeros lie on $x = 1/2$, the eigenvalues themselves remain mysterious, making it difficult to form a portrait of $Z(s)$ in \mathbb{C} . For example the 1st and 3rd eigenvalues computed numerically are $\lambda_1 = 91.14$, $\lambda_3 = 190.13$, giving pairs of zeros at $1/2 \pm 9.533i$ and $1/2 \pm 13.779i$ respectively, but there are no closed classical mathematical formulae.

A very different approach to the Selberg zeta function developed by Mayer uses the transfer operator. Given a space of holomorphic functions V on an open disc, he defines an operator

$L_s : V \rightarrow V$ by the formula $L_s \phi(z) = \sum_{n=1}^{\infty} \frac{1}{(z+n)^{2s}} \phi\left(\frac{1}{z+n}\right)$, $\phi \in V$, $z \in D$. This converges for

$\text{Re}(s) > 1/2$ any $\phi \in V$ and can be continued meromorphically to \mathbb{C} . As this is a finite sum of Hurwitz zeta functions, it has an accessible analytic continuation, and has 'nuclear' eigenvalues (converging rapidly to zero) and in particular L_s is trace class (having a well-defined finite trace – i.e. there are only countably many non-zero eigenvalues and their sum is well defined), and has a determinant in the Fredholm sense (a complex function generalizing the notion of determinant), making it possible to express the zeta functions of $\Gamma = SL(2, \mathbb{Z})$ and $\Gamma_+ = GL(2, \mathbb{Z})$ as a determinant: $Z_\Gamma(s) = \det(1 - L_s^2)$, $Z_{\Gamma_+}(s) = \det(1 - L_s)$.

These methods are computationally intensive because they involve defining matrices of ever expanding dimensions to capture and sort the eigenvalues to define the zeta function.

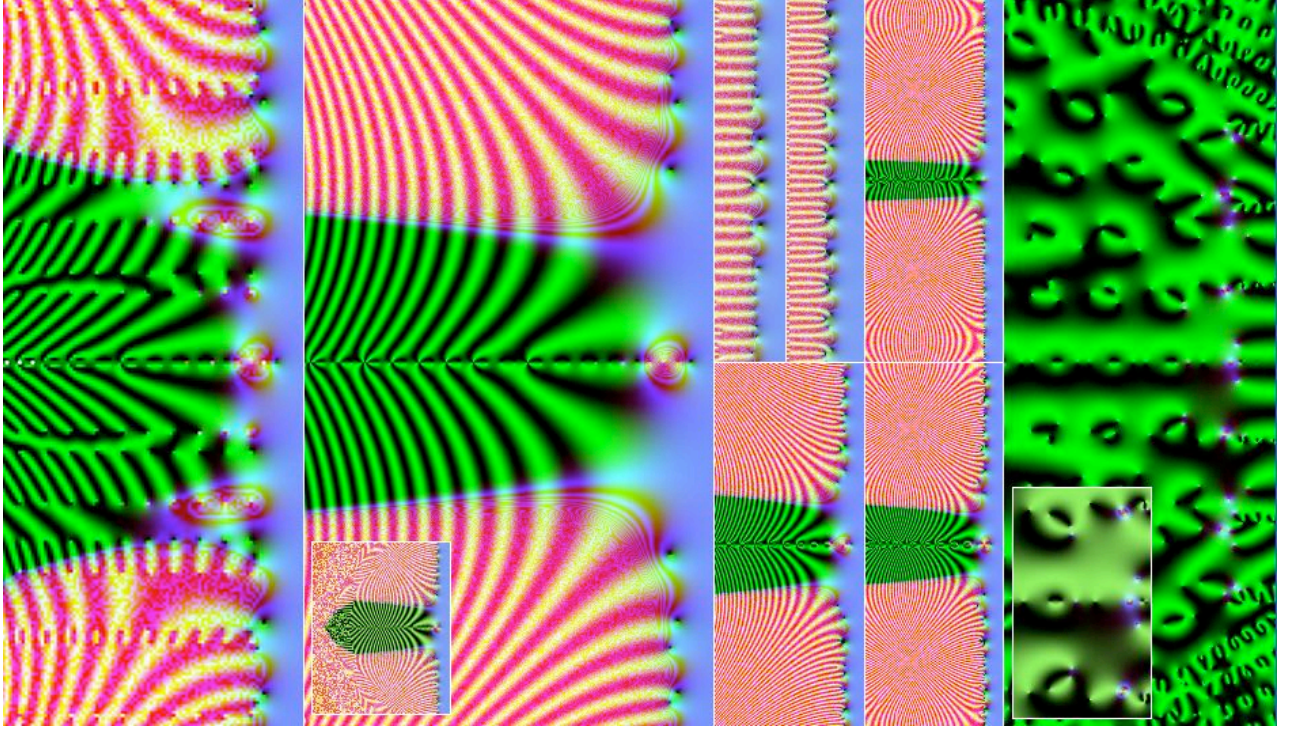


Fig 7: Selberg zeta function portraits. Left: Selberg zeta function of Hecke triangle group $G(3)$ $-8.2 \leq x \leq 1.8$ $|y| \leq 13.4$ (Stromberg) showing a complicated profile with strings of zeros and poles at integer x values associated with some non-trivial zeros. These are further highlighted in figs 8 and 8b. Centre: Selberg zeta function for $\Gamma = SL(2, \mathbb{Z})$ $-13.2 \leq x \leq 1.8$ $|y| \leq 13.4$ (Fraczek) with five times larger scale portrait inset showing the full central basin. Centre right: (Above) Zeta functions for the tri-funnel and funnel-torus $-3.2 \leq x \leq 1.8$ $|y| \leq 6.7$ (Borthwick) do not include specific algorithms for analytic continuation. (Below) Selberg zeta function of $\Gamma_0(2)$ $-8.2 \leq x \leq 1.8$ $|y| \leq 13.4$ (Fraczek) Right: (Above) First parameter deformation of $\Gamma_0(4)$ (Below) unmodified $\Gamma_0(4)$ Right: Selberg zeta function of the Kac-Baker model $-41 \leq x \leq 18$ $|y| \leq 67$ of systems with weak long-range interactions such as a van der Waals gas. See also figs 8 and 14 for comparisons.

Markus Fraczek's algorithm illustrated in fig 7 uses the transfer operator approach to generate a high resolution algorithm for the analytic continuation of the Selberg zeta functions of $SL(2, \mathbb{Z})$ and $\Gamma_0(n)$ for $n = 2, 4, 8$, exploring character deformations for $n = 4, 8$. His 'widmo' command line algorithm runs in a unix C-environment optimally compiled for a given machine so the general outlines of the method are summarized here from his thesis.

$$\text{A character } \chi_{\alpha_1, \dots, \alpha_k}^\Gamma : \Gamma \rightarrow \mathbb{C} \text{ for a freely generated group } \Gamma \text{ is given by } \chi_{\alpha_1, \dots, \alpha_k}^\Gamma(\gamma) = \exp 2\pi i \sum_{i=1}^k \alpha_i \Omega_i^\Gamma(\gamma)$$

$$\text{where } k \text{ is the number of generators of } \Gamma, 0 \leq \alpha_i \leq 1, \text{ and } \Omega_i^\Gamma : \Gamma \rightarrow \mathbb{Z} \text{ is given by } \Omega_i^\Gamma(\gamma) = \sum_{j=1}^N n_{i,j},$$

$$\text{where } N = N(\gamma) \text{ and } n_{i,j} = n_{i,j}(\gamma) \text{ are given by } \gamma = \prod_{j=1}^N (G_1^\Gamma)^{n_{1,j}} (G_2^\Gamma)^{n_{2,j}} \dots (G_k^\Gamma)^{n_{k,j}}$$

The transfer operator is defined using a close orbit equivalence between the group transformations of $\Gamma(n)$ and a chaotic discrete mapping characterized by symbolic dynamics.

The symbolic dynamics of the geodesic flow on $\Gamma \backslash \mathbb{H}$ can be described by the Poincaré map

$$P_\Gamma : [0, 1] \times [0, 1] \times \{+1, -1\} \times \Gamma \backslash \mathrm{SL}(2, \mathbb{Z}) \rightarrow [0, 1] \times [0, 1] \times \{+1, -1\} \times \Gamma \backslash \mathrm{SL}(2, \mathbb{Z})$$

$$\text{given by} \quad P_\Gamma(x, y, \varepsilon, \Gamma g) = \left(T_G(x), \left(y + \left[\frac{1}{x} \right] \right)^{-1}, -\varepsilon, \Gamma g T^{\varepsilon \left[\frac{1}{x} \right]} S \right).$$

The expanding part of this map determining the ergodic properties, is given by

$$P_{\Gamma, \text{ex.}}(x, \varepsilon, \Gamma g) = \left(T_G(x), -\varepsilon, \Gamma g T^{\varepsilon \left[\frac{1}{x} \right]} S \right).$$

To construct the transfer operator we need the inverse branches of this map, given by

$$P_{\Gamma, \text{ex.}}^{-1}(x, \varepsilon, \Gamma g) = \left\{ \left(\frac{1}{x+l}, -\varepsilon, \Gamma g S T^{\varepsilon l} \right) : l \in \mathbb{Z}_> \right\}.$$

The transfer operator for the geodesic flow on $\Gamma \backslash \mathbb{H}$ has the form

$$\tilde{\mathcal{L}}_\beta = \begin{pmatrix} 0 & \mathcal{L}_{\beta, +1} \\ \mathcal{L}_{\beta, -1} & 0 \end{pmatrix},$$

where $\mathcal{L}_{\beta, \varepsilon} : \bigoplus_{i=1}^\mu B(D) \rightarrow \bigoplus_{i=1}^\mu B(D)$ is given by

$$\mathcal{L}_{\beta, \varepsilon} \vec{f}(z) = \sum_{l=1}^\infty (z+l)^{-2\beta} U^\Gamma(S T^{\varepsilon l}) \vec{f}\left(\frac{1}{z+l}\right), \quad \text{for } \Re \beta > \frac{1}{2}$$

with $\vec{f}(z) = (f_i(z))_{1 \leq i \leq \mu}$, and $\mu = [\mathrm{SL}(2, \mathbb{Z}) : \Gamma]$ the index of Γ in $\mathrm{SL}(2, \mathbb{Z})$.

The Selberg zeta function is again defined in terms of the Fredholm determinant:

$$Z(\beta) = \det(1 - \tilde{\mathcal{L}}_\beta) = \det(1 - \mathcal{L}_{\beta, +1} \mathcal{L}_{\beta, -1}) = \det(1 - \mathcal{L}_{\beta, -1} \mathcal{L}_{\beta, +1}).$$

The Selberg zeta functional equation is extended to cover the character deformations:

$$\varphi(\beta, \chi) Z(\beta, \chi) = \eta(\beta) Z(1 - \beta, \chi)$$

$$\text{with} \quad \eta(\beta) = \eta\left(\frac{1}{2}\right) \left(2^{2\beta-1} \frac{\Gamma\left(\frac{1}{2} + \beta\right)}{\Gamma\left(\frac{3}{2} - \beta\right)} \right)^{h_0} \exp \left\{ \frac{\pi}{3} \mu_n \int_0^{\beta - \frac{1}{2}} \tau \tan(\pi \tau) d\tau \right\} \prod_{\chi(T_i) \neq 1} |1 - \chi(T_i)|^{2\beta-1},$$

$$\eta\left(\frac{1}{2}\right) = \pm 1. \text{ Furthermore, we have } \eta(\beta) \eta(1 - \beta) = 1.$$

If the number h_0 of open cusps vanishes then $\varphi(\beta, \chi)$ is absent.

A direct analytic continuation is also provided for the transfer operator with character deformation. Fraczek's analytic continuation involves the Lerch transcendent, a generalization of the Hurwitz zeta function, noted above.

Lemma 7.4.6. *The analytic continuation of the transfer operator in lemma 7.4.5 is given for*

$\Re \beta > -\frac{N}{2}$, $N \in \mathbb{Z}_>$, by

$$\left[\mathcal{L}_{\beta, \varepsilon, \chi}^{(n)} \vec{f}(z) \right]_i = \left[\mathcal{N}_{\beta, \varepsilon, \chi, N}^{(n)} \vec{f}(z) \right]_i + \left[\mathcal{A}_{\beta, \varepsilon, \chi, N}^{(n)} \vec{f}(z) \right]_i$$

$$\text{where} \quad \left[\mathcal{N}_{\beta, \varepsilon, \chi, N}^{(n)} \vec{f}(z) \right]_i = \sum_{q=0}^\infty \sum_{m=1}^n \sum_{j=1}^{\mu_n} [U^\chi(S T^{m\varepsilon})]_{i,j} \chi \left(r_j^{(n)} T^{n\varepsilon} (r_j^{(n)})^{-1} \right)^q \left[(z+m+nq)^{-2\beta} f_j \left(\frac{1}{z+m+nq} \right) - \sum_{k=0}^N (z+m+nq)^{-2\beta-k} \frac{f_j^{(k)}(0)}{k!} \right]$$

$$\text{and} \quad \left[\mathcal{A}_{\beta, \varepsilon, \chi, N}^{(n)} \vec{f}(z) \right]_i = \sum_{m=1}^n \sum_{j=1}^{\mu_n} [U^\chi(S T^{m\varepsilon})]_{i,j} \sum_{k=0}^N \frac{f_j^{(k)}(0)}{k!} \frac{1}{n^{2\beta+k}} \Phi \left(\chi \left(r_j^{(n)} T^{n\varepsilon} (r_j^{(n)})^{-1} \right), 2\beta+k, \frac{z+m}{n} \right).$$

The Lerch transcendent is defined as $\Phi(\alpha, s, z) = \sum_{n=0}^\infty \alpha^n (z+n)^{-s}$

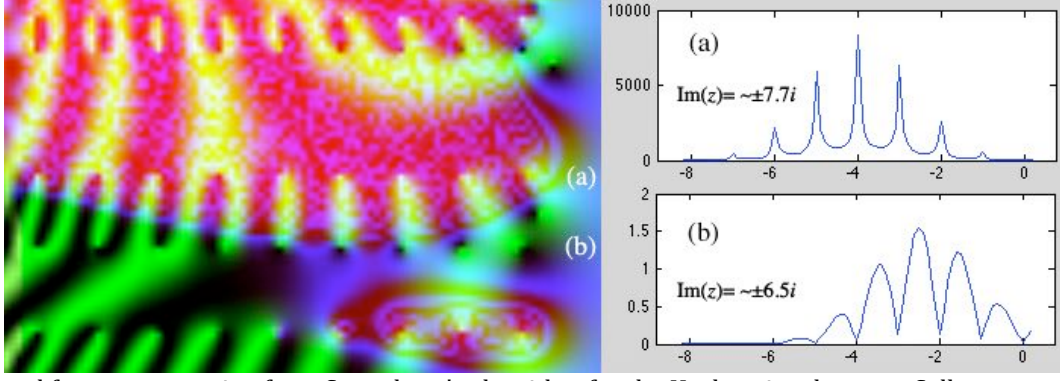


Fig 8: Novel features emerging from Stromberg's algorithm for the Hecke triangle group Selberg zeta function, including further strings of zeros and poles associated with imaginary values related to the non-trivial zeros.

Fredrik Stromberg's Hecke triangle group zeta function has new features not apparent in the $SL(2, \mathbb{Z})$ and $\Gamma_0(2)$ cases, with in addition to the poles at negative half-integer values and zeros at negative integer values on the real axis, further strings of zeros and poles associated with imaginary values related to the non-trivial zeros.

The algorithm for Hecke triangle groups likewise uses transfer operators defined by symbolic dynamics almost orbit equivalent to the group action and defines the zeta function via Fredholm determinants.

If $\{x\}_\lambda = \lfloor \frac{x}{\lambda} + \frac{1}{2} \rfloor$ is a nearest λ -multiple function we define $F_q : I_q \rightarrow I_q$ by $F_q(0) = 0$ and $F_q(x) = -\frac{1}{x} - \{x\}_\lambda \lambda$ for $x \neq 0$. For any number $x \in \mathbb{R}$ we obtain the regular λ -fraction of x , $c_q(x) = [a_0; a_1, a_2, \dots]$ by first setting $a_0 = \{x\}_\lambda$, $x_1 = x - a_0 \lambda$, and then recursively set $a_n = \{Sx_n\}_\lambda$ and $x_{n+1} = F_q(x_n)$ for $n \geq 1$. F_q is almost orbit equivalent to G_q ,

$$\mathcal{L}_\beta f(x) = \sum_{y \in F_q^{-1}(x)} \left| \frac{d}{dx} F_q^{-1}(x) \right|^\beta f(y(x))$$

If $A = \begin{pmatrix} a & b \\ c & d \end{pmatrix} \in PSL_2(\mathbb{R})$ and $A(D) \subseteq D$ for some disk D then $\pi_\beta(A) : \mathcal{B}(D) \rightarrow \mathcal{B}(D)$ is defined for any $\beta \in \mathbb{C}$ by $\pi_\beta(A) f(z) = \left((cz + d)^{-2} \right)^\beta f\left(\frac{az+b}{cz+d}\right)$.

Let $\mathcal{B}(x) = \mathcal{B}(D_j)$ where $x \in D_j$, set $A_r r = r$ and $\mathcal{K}_\beta = \pi_\beta(A_r)$.

$$\det(1 - \mathcal{L}_\beta) = \sum_{l=1}^{\infty} \frac{1}{l} \text{Tr} \mathcal{L}_\beta^l = \sum_{l=1}^{\infty} \frac{1}{l} \sum_{[n_1, n_2, \dots, n_l] \in \mathcal{S}_l} \frac{\mathcal{N}(A_{\vec{n}})^{-\beta}}{1 - \mathcal{N}(A_{\vec{n}})^{-1}}$$

$$Z_q(\beta) = \frac{\det(1 - \mathcal{L}_\beta)}{\det(1 - \mathcal{K}_\beta)}.$$

Stromberg provides a standard functional equation for zeta, but his algorithm calculates zeta directly and uses the values of $Z(s)$ and $Z(1-s)$ to calculate the scattering matrix.

The functional equation Let $Z_q(s)$ be the Selberg Zeta function for G_q .

$$\frac{Z_q(1-s)}{Z_q(s)} = \varphi_q(s) c \Psi_q(s),$$

where $\varphi_q(s)$ is the scattering matrix (here a 1×1 -matrix), $c = \varphi_q\left(\frac{1}{2}\right) = \pm 1$ and

$$\Psi_q(s) = \frac{\Gamma\left(\frac{3}{2}-s\right)}{\Gamma\left(s+\frac{1}{2}\right)} \exp\left(-\frac{q-2}{q} \pi \int_0^{s-\frac{1}{2}} t \tan(\pi t) dt + \pi \sum_{k=1}^{q-1} \frac{1}{q \sin \frac{k\pi}{q}} \int_0^{s-\frac{1}{2}} \left(\frac{e^{-\frac{2\pi i k t}{m}}}{1+e^{-2\pi i t}} + \frac{e^{\frac{2\pi i k t}{m}}}{1+e^{2\pi i t}} \right) dt + (1-2s) \ln 2\right).$$

He provides an analytic continuation for the transfer operator using Hurwitz zeta functions.

$$\begin{aligned}
\mathcal{L}_{\beta, iK} f(z) &= \sum_{n \in \mathcal{N}_{iK}} \pi_{\beta}(ST^n) f(z) = \sum_{n \geq n_{iK}} \pi_{\beta}(ST^n) f(z) \\
&= \sum_{n \geq n_{iK}} \left(\frac{1}{z+n\lambda} \right)^{2\beta} f\left(\frac{-1}{z+n\lambda} \right) \\
&= \sum_{n \geq n_{iK}} \left(\frac{1}{z+n\lambda} \right)^{2\beta} \left[\sum_{k=0}^N a_k \left(\frac{-1}{z+n\lambda} \right)^k + R_N \left(\frac{1}{z+n\lambda} \right) \right] \\
&= \mathcal{A}_{\beta, iK}^{(N)} f(z) + \mathcal{L}_{\beta, iK}^{(N)} f(z)
\end{aligned}$$

where $\mathcal{L}_{\beta, iK}^{(N)} f(z) = \mathcal{L}_{\beta, iK} [f(z) - \sum_{k=0}^N a_k z^k]$ is analytic for $\Re \beta > \frac{1-N}{2}$ and in fact nuclear of order 0. We also have $\left\| \mathcal{L}_{\beta, iK}^{(N)} f(z) \right\|_{\infty} \leq C \sum_{n \geq n_{iK}} \left| \frac{1}{n\lambda} \right|^{2\Re \beta + N + 1} \rightarrow 0$ as $N \rightarrow \infty$. The operator $\mathcal{A}_{\beta, iK}^{(N)}$ on the other hand can be written as

$$\begin{aligned}
\mathcal{A}_{\beta, iK}^{(N)} f(z) &= \sum_{k=0}^N (-1)^k a_k \sum_{n \geq n_{iK}} \left(\frac{1}{z+n\lambda} \right)^{2\beta+k} \\
&= \sum_{k=0}^N (-1)^k a_k \lambda^{-2\beta-k} \zeta \left(2\beta+k, \frac{z}{\lambda} + n_{iK} \right)
\end{aligned}$$

where $\zeta(s, z)$ is the Hurwitz zeta function.

Stromberg's open source MuPad code released under GNU GPL v2 is added as an appendix, so it is possible to trace exactly how the algorithm generates the zeta function in this case.

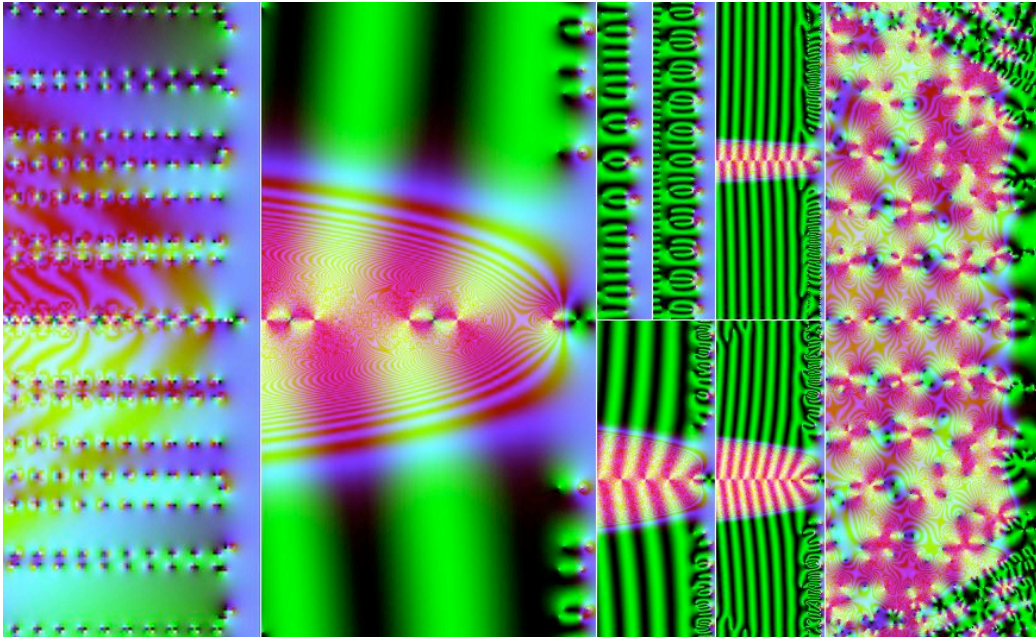


Fig 8b: The zeta functions $\zeta(s) = Z(s+1)/Z(s)$ corresponding to the Z functions of Fig 7 highlight changes in the argument associated with zeros and poles.

(d) Dynamical Zeta Functions

Coming full circle, for a set of Mobius maps such as the Schottky group of the tri-funnel (Pollicott 2013), we can consider the Ruelle transfer operator $\mathcal{L}_s : B \rightarrow B$, where B is a Banach space (a complete normed vector space) defined likewise on a small open complex neighbourhood by $\mathcal{L}_s w(z) = \sum_{g \neq g_0} e^{-s \log |T_g'(z)|} w(T_g(z))$, $z \in I(g_0)$. Where the I 's are the isometric circles linking the Mobius maps. Again the operator and its powers are trace class and we

have $trace(L_s^n) = \sum_{g=g_1 \cdots g_n} \frac{e^{-s \log |T_g'(x(g))|}}{1 - |T_g'(x(g))|}$ and can define the Ruelle zeta function as

$$Z(s) = \exp \left(- \sum_{n=1}^{\infty} \frac{1}{n} trace(L_s^n) \right) = \prod_{n=1}^{\infty} e^{-trace(L_s^n)/n}, \text{ echoing the matrix definition of trace:}$$

$$\frac{1}{\det(I - A)} = \exp \left(- \sum_{n=1}^{\infty} \frac{1}{n} trace(A^n) \right), \quad trace(A) = \sum_{i=1}^n a_{i,i}.$$

The Ruelle zeta function can in turn be extended to Anosov flows – topologically transitive (mapping any small open set eventually over any other) chaotic flows on manifolds of varying negative curvature, containing a single dense orbit (Policott). In the compact case where orbits have to recycle in the space hyperbolicity effectively guarantees chaotic dynamics.

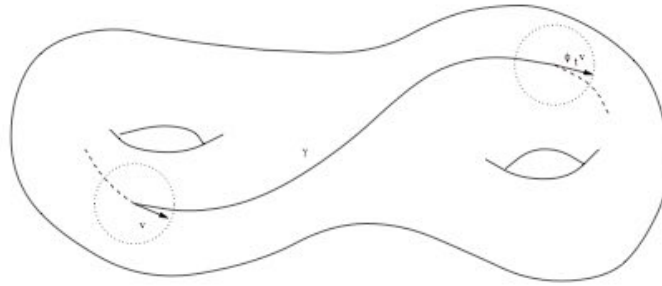


Fig 9: The geodesic flow on a negatively curved surface is an example of an Anosov flow.

The Kac-Baker model illustrated in fig 7 provides an example of a dynamical zeta function, lying outside the domain of arithmetic zeta functions, with very different properties from the Selberg zeta functions already discussed. It describes a 1-dim. classical lattice spin system with an exponentially decaying two body interaction, developed to investigate phase transitions in systems with weak long-range interactions such as a van der Waals gas. Ruelle's dynamical zeta function for this model can be expressed in terms of Fredholm determinants of two transfer operators and hence is a meromorphic function.

The transfer operator $\mathcal{L}_{\beta,\lambda} : B(D_R) \rightarrow B(D_R)$, given by

$$\mathcal{L}_{\beta,\lambda} f(z) = e^{\beta z} f(\lambda + \lambda z) + e^{-\beta z} f(-\lambda + \lambda z)$$

The trace of this operator is given by $\text{tr } \mathcal{L}_{\beta,\lambda} = \frac{2}{1-\lambda} \exp \frac{\beta \lambda}{1-\lambda}$.

The Ruelle zeta function (7.4) for the Kac-Baker model has the representation

$$Z_R(z, \beta) = \frac{\det(1 - z \lambda \mathcal{L}_{\beta,\lambda})}{\det(1 - z \mathcal{L}_{\beta,\lambda})} \quad \text{for } z, \beta \in \mathbb{C}.$$

As soon as the eigenvalues $\rho_i = \rho_i(\beta, \lambda)$ of $\mathcal{L}_{\beta,\lambda}$ are known, $Z_R(\beta) = \frac{\prod_{i=0}^{\infty} 1 - \lambda \rho_i}{\prod_{i=0}^{\infty} 1 - \rho_i}$.

For $0 < \lambda < 1$ the Fredholm determinants $\det(1 - \lambda \mathcal{L}_{\beta,\lambda})$ and $\det(1 - \mathcal{L}_{\beta,\lambda})$ have infinitely many zeros on the real line $\beta \in \mathbb{R}$. Furthermore, the Fredholm determinant $\det(1 - \lambda \mathcal{L}_{\beta,\lambda})$ also has infinitely many zeros on the line $\text{Re } \beta = \ln 2$.

Hilgert and Mayer note that:

1. The zeros on the line $\text{Re}\beta = \ln 2$ are equally spaced and given by $\beta = \ln 2 + i2\pi n$ with $n \in \mathbb{Z}$. It has been concluded that the Ruelle zeta function $R(\beta) := Z(1, \beta)$ has infinitely many zeros and poles on the real line, and for the special value $\lambda = 1$ infinitely many trivial zeros on the line $\text{Re}\beta = \ln 2$.
2. Accidental cancellations of the zeros of $\det(1 - \lambda L_{\beta, \lambda})$ with the zeros of $\det(1 - L_{\beta, \lambda})$ could destroy some of these zeros in $Z(\beta)$

They raise two questions:

1. Does the Ruelle zeta function $Z(\beta)$ also have zeros on a line parallel to the imaginary β -axis for $0 < \lambda < 1$ different to $\lambda = 1$?
2. Are there any other zeros of the Ruelle zeta function $Z(\beta)$ which are neither on the line $\text{Re}\beta = \ln 2$ nor on the real line $\beta \in \mathbb{R}$ for $\lambda = 1$?

It is expected that there are zeros on lines parallel to the imaginary β -axis for all values for λ . On the other hand, if at least for $\lambda = 1$ there are only zeros on the line $\text{Re}\beta = \ln 2$ and on the real axis, then some general Riemann hypothesis would also hold for the zeta function $Z(\beta)$. Indeed, there is no obvious connection of this zeta function to any arithmetic zeta function for which such a general Riemann hypothesis is known to hold.

Fraczec comments: "Comparing the Ruelle zeta function $Z(\beta)$ to other zeta functions we have computed during other numerical investigations in this thesis, shows that this zeta function is somehow different from the others: The absolute value of $Z(\beta)$ is rather small and we do not see any strong oscillation of the real part and the imaginary part of $Z(\beta)$ which seems to be typical for all other zeta functions. The zeta function $Z(\beta)$ appears to be quite regular in the β plane. Furthermore, the zeros and poles of $Z(\beta)$ have some pattern in the β -plane which is not very striking, and the parameter λ acts almost just as a scaling parameter of the β -plane. Also, the zeros and the poles have presumably not any deep interpretation like in the case of, e.g., Selberg zeta function. Moreover, there is a vast amount of information encoded in the Selberg zeta function; this seems not to be the case for the function $Z(\beta)$. Indeed, it might be that the Ruelle zeta function $Z(\beta)$ and maybe even general dynamical zeta functions are somehow different to the 'classical' arithmetic zeta functions."

Coming Back for Real-World Air: Physics and the Zeta Functions

Because the integers underlie our numerical understanding of the universe, any physical system involving primes or relatively prime integers can invoke the Riemann zeta function.

Our first example involves counting finite orbit escapes in a circular stadium with small slits (fig 11). This leads to probabilities invoking Euler's totient and the Mobius function, because a periodic orbit in n steps requires angle $\psi = \pi / 2 - m\pi / n$, for $m < n$ and relatively prime. The Mellin transform governing the leading order then becomes a function of the non-trivial zeros of $\zeta(1 + s)$. One can thus use the deviation of the second order terms as an experimental test of the Riemann hypothesis (Bunimovich & Dettmann 2005).

Next consider a non-relativistic, non-interacting, spin zero Bose gas of dimension D . This system undergoes a phase transition at low temperatures, where the de-Broglie wavelength of the particles becomes comparable to the inter-particle distance, so that the quantum nature of the constituents becomes decisive. Since the particles are free, their spectrum is

continuous, equal to the kinetic energy $E = p^2 / 2m$. The total number of particles N is the sum of particles in each quantum state: $N = \frac{1}{h^D} \int f_{BE}(E(p)) d^D q d^D p = \frac{V}{h^D} \int \frac{d^D p}{e^{(E(p)-\mu)/kT} - 1}$.

Changing the integration from momentum to energy gives $N \propto \int_0^\infty \frac{E^{D/2-1}}{e^{(E-\mu)/kT} - 1} dE \propto \zeta\left(\frac{D}{2}\right)$.

Therefore the Bose-Einstein condensation phase transition cannot occur in homogeneous non-interacting systems in dimensions lower than three, since the total number of atoms is positive and fixed for our system, but in one spatial dimension, since $\zeta(1/2) < 0$ N appears negative, and in two-dimensions N appears to be infinite because $\zeta(1)$ is a pole. The involvement of zeta continues in more complex Bose gas models, including other transitions e.g. of heat capacity and the number fluctuation of an ideal gas (Schumayer & Hutchinson 2011), leading to the suggestion that a Bose-Einstein condensate could in theory be used to factorize numbers as a quantum computer calculating prime factors (Weiss et al., 2004). LeClair (2013) has used a careful analysis of the 2-dimensional case to claim from the thermal statistics that the Riemann hypothesis must hold.

(a) Gutzwiller's Semiclassical Trace Formula

We have seen that the derivation of the Ruelle zeta function and its use of the transfer operator in Selberg zeta functions has arisen from an application of thermodynamic principles to chaotic flows in hyperbolic space. Higher dimensional hyperbolic space is intrinsic to cosmology where de Sitter space figures in the holographic principle of supergravity theories (Maldacena 1998, Maldacena and Susskind 2013). The extension of Selberg zeta functions to higher dimensional hyperbolic spaces including n -dimensional hyperbolic cylinders has been used in the description of black hole thermodynamics (Williams 2003, 2010). We shall also later explore superstring theories and zeta functions.

More generally the Selberg trace formula became a model for relating the eigenvalues typical of quantum wave function methods to the unstable repelling orbits in the classical versions of quantum chaos. Using this relationship, Martin Gutzwiller (1971) developed a trace formula to express the eigenvalues of a chaotic quantum system in terms of the closed classical orbits in the semi-classical limit as $\hbar \rightarrow 0$. His trace formula is very different from Selberg's, being based on the Greens function propagators of the classical orbits. Summarized as briefly as possible we have the following.

The semi-classical Green's function is obtained by Fourier transform of the propagator:

$$\begin{aligned} G_{sc}(\mathbf{r}, \mathbf{r}', E) &= -\frac{2\pi i}{h} \int_0^\infty \exp\left(\frac{2\pi i}{h} Et\right) K_{sc}(\mathbf{r}, \mathbf{r}', t) dt \\ &= -\frac{2\pi i}{h} \left(\frac{1}{ih}\right)^{d/2} \sum_{class. paths} \int_0^\infty \exp\left(\frac{2\pi i}{h} [R(\mathbf{r}, \mathbf{r}', t) + Et] - i\mu \frac{\pi}{2}\right) |D_{\mathbf{r}, \mathbf{r}'}|^{1/2} dt \end{aligned}$$

The trace of the Greens function is

$$\tilde{G}(E) = -\frac{2\pi i}{h} \left(\frac{1}{ih}\right)^{(d+1)/2} \sum_{class. paths} \int_0^\infty \exp\left(\frac{2\pi i}{h} S(\mathbf{r}, \mathbf{r}', E) - i\mu \frac{\pi}{2}\right) |D|^{1/2} d\mathbf{r}$$

Gutzwiller's semi-classical approximation becomes

$$G_{scl}(\mathbf{r}, \mathbf{r}', E) = -\frac{2\pi i}{h} (ih)^{-(d+1)/2} \sum_{class. paths} \int_0^\infty \exp\left(\frac{2\pi i}{h} S(\mathbf{r}, \mathbf{r}', E) - i\mu \frac{\pi}{2}\right) |D|^{1/2} d\mathbf{r}$$

$$D(\mathbf{r}, \mathbf{r}', E) = (-1)^{(d+1)} \begin{vmatrix} \frac{\partial^2 S}{\partial \mathbf{r}' \partial \mathbf{r}} & \frac{\partial^2 S}{\partial \mathbf{r}' \partial E} \\ \frac{\partial^2 S}{\partial E \partial \mathbf{r}} & \frac{\partial^2 S}{\partial E^2} \end{vmatrix}$$

His trace formula then expresses the oscillating part of the level density in terms of isolated periodic orbits

$$\delta g_{scl}(E) = \frac{2}{h} \sum_{po} \frac{T_{ppo}}{\sqrt{|\det(\tilde{M}_{po} - I)|}} \cos\left(\frac{2\pi}{h} S_{po} - \sigma_{po} \frac{\pi}{2}\right), \sigma_{po} = \mu_{po} + \nu_{po} \text{ Maslov index}$$

S_{po} : action along the orbit, $T_{ppo} = \frac{\partial S_{po}}{\partial E}$: orbit period, \tilde{M}_{po} : stability matrix

Gutzwiller's trace formula has since become a means to compare the eigenfunctions of quantum chaos with the semi-classical approach using the repelling closed orbits of the corresponding systems, giving a description of diverse phenomena in quantum chaos, from scarring of the wave function, through asymptotic periodicity emerging from transient irregularity in quantum systems, to the energy separation of the energy levels in chaotic systems such as Wigner's spectrum of the atomic nucleus (Gutzwiller 1992).

Some of these systems can be made to fit the Selberg zeta function exactly. Sieber and Steiner (1992) were able to produce the eigenvalues of the quantum hyperbolic Sinai billiard (fig 10) to high resolution from the zeros of the Selberg zeta function. Following on from this Keating and Sieber (1994) produced spectral determinants for the hyperbolic quantum billiard. Eckhardt et al. (1995) were likewise able to analyse the quantum Selberg zeta function of three disc quantum pinball and outline the nature of its zeros and poles in a similar manner to the Kac-Baker zeta function above.

(b) Quantum Suppression of Chaos and Classical Orbits

The quantum stadium (fig 10) is a direct analogue of the classical chaotic stadium billiard, which displays the classical butterfly effect of chaos - sensitive dependence on initial conditions - and for almost all orbits produces a dense trajectory filling the stadium. Within this classical system is a dense set of repelling periodicities, any arbitrarily small deviation from which results in a dense orbit, or a differing unstable periodicity.

The quantum versions of this system behave in a fundamentally different manner. While the initial stages of a trajectory follow the classical picture, after a limited period of time, called the quantum break time, they have a cumulatively increasing probability of entering one of the eigenvalues of the system. These eigenvalues turn out to correspond to the closed orbits of the classical system, which have now become probability maxima of the quantum system because wave spreading has effectively compensated for sensitive instability of the orbit, resulting the so-called scarring of the quantum wave function by probability maxima along these closed orbits. These also extend to fractal eigenstates of open chaotic systems (Casati et. al 1999).

Moreover, unlike the eigenvalues of ordered quantum systems such as the Lyman, Balmer and Paschen series of orbital electrons, whose energy separation converges to zero at infinity, the chaotic eigenvalues display energy separation statistically distributed as a Gaussian orthogonal or

unitary ensemble (GOE or GUE) suppressing small energy transitions between eigenvalues. Semi-classical simulations of such systems, using a small classical wave packet, generally give similar results, showing the suppression of chaos and the separation of eigenvalues is directly caused by wave spreading. Nevertheless for some quantum systems with chaotic dynamics, such as the GUE and GOE statistics of nuclear energetics, the classical system is ordered. Although rectangular and circular stadia have ordered classical dynamics, the nuclear statistics of the quantum potential well is chaotic. The quantum stadium differs from the hyperbolic billiard because the classical flow is ergodic (randomly space filling) but not Anosov (uniformly hyperbolic), so its orbit distribution can be different and potentially more complex (fig 10).

In systems like the quantum stadium, the closed orbits playing a role similar to the primes in that they are orthogonal, i.e. uncoupled to one another, are determined by constraints which result in a discrete spectrum and form an irrationally related subset of the phase space. Primes among the numbers behave similarly in that they have no common factors, form a discrete spectrum having no consistent rational formulation and act as a set of discrete generators of all the other integers. Thus the correspondence may be analogical but not homologous.

The end result is that for a variety of closed quantum systems, wave spreading eventually represses classical chaos by scarring, causing the periodic eigenfunctions to become eventual solutions of the time-dependent problem, although the initial trajectory behaves erratically, just as does an orbit in the classical situation. For example, a periodically kicked quantum rotator (Moore et. al 1995, Raizen et al. 1996) will stochastically gain energy, just as in the classical situation, until a quantum break time (Berry 1989), after which it will become trapped in one of the quantum solutions. A highly excited atom in a magnetic field will have absorbance peaks at the periodic solutions, and quantum tunneling will likewise use scarred eigenvalues as its principle modes of tunneling (Gutzwiller 1992). However if a kicked rotator in a chaotic state is able to interact with other processes, such as nuclear spin, it can become quantum entangled and thus form a more complicated system (Chaudury et al. 2009, Steck 2009).

(c) The GUE and Zeta Statistics

A breakthrough concerning the zeros of the Riemann zeta function was thought to have happened when Hugh Montgomery (1973) made contact with the physicists studying nuclear energy levels at Princeton and found that the pair correlations in the gaps between the Riemann zeta zeros he had discovered followed the same Gaussian unitary ensemble statistics as chaotic quantum systems and energy levels of large nuclei:

$$\sum_{\substack{\frac{2\pi\alpha}{\log T} \leq \gamma' - \gamma \leq \frac{2\pi\beta}{\log T}}} 1 \sim N(T) \int_{\alpha}^{\beta} \left(1 - \left(\frac{\sin \pi u}{\pi u} \right)^2 \right) du$$

The GUE statistic and its time-reversible real variant, the GOE, or Gaussian orthogonal ensemble, appear in many forms of quantum system whose classical analogue is chaotic. The corresponding form for fermions, rather than bosons is the symplectic GSE. These include both the many body problem of nuclear energetics, highly excited atoms in a magnetic field and the quantum stadium problem. One of the high moments in this interaction of fields was the Keating's development of a formula for the Riemann zeta moments, using characteristic polynomials of unitary matrices.

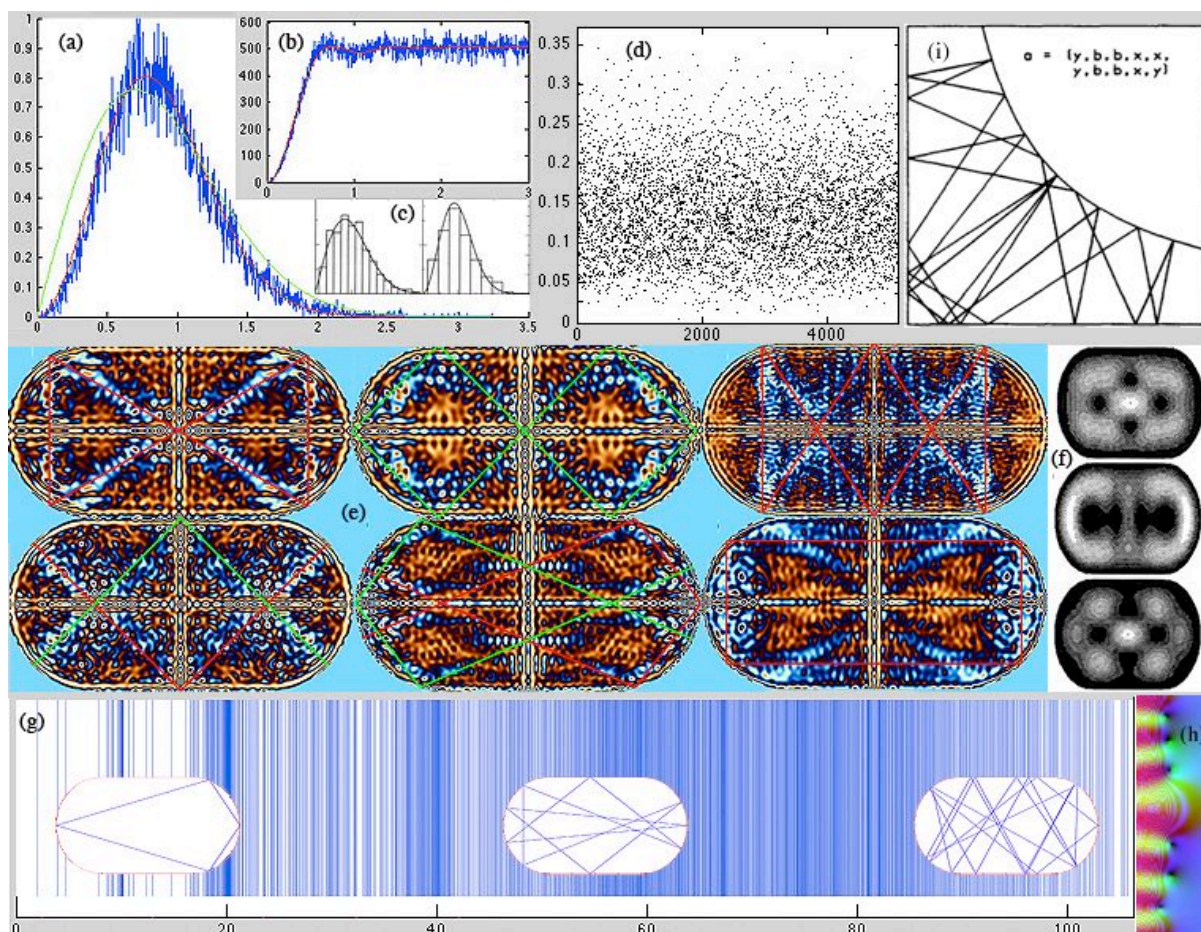


Fig 10: The Quantum Chaos connection. (a): The spacing between zeta zeros 100-10,000 is compared with a Gaussian Unitary Ensemble distribution $32\pi^{-2}s^2e^{(-4s^2/\pi)}$ (red), showing coincidence of the two statistics, and a Gaussian Orthogonal Ensemble $\pi se^{(-\pi s^2)}/2$ (green) characteristic of the Wigner distribution of atomic nuclear energies. (b) Pair correlations for the first 10^5 zeros compared with the theoretical GUE distribution. (c) Eigenvalues of quantum dot stadium wave function (f) (Liu et al. 1998) display both GOE and GUE forms of random matrix distribution under increasing magnetization of the electron's orbit. (d) Pattern of differences between successive zeros of zeta in the range from 10^{21} for 10^4 successive zeros determined by Odlyzko shows a Hurst exponent corresponding to a fractal dimension of 1.9 with pronounced negative persistence, differing significantly from corresponding statistics of GUE random matrices. (e) The quantum stadium potential well shows 'scarring' of the wave function along classical repelling orbits, thus repressing the classical chaos, through probabilities clumping on the repelling orbits. The cellular automaton wave simulation shows why this is so (King 2009a). A small wavelet bounces back and forth, forming a periodic wave pattern, because even when slightly off the repelling orbit the wave still overlaps itself and can form standing wave constructive interference when its energy and frequency corresponds to one of the eigenvalues of a periodic orbit. (g) The classical stadium billiards is chaotic. The stadium is densely filled with repelling periodic orbits, three of which are shown with increasing orbit length. The spectrum of orbit lengths has a complex fractal character somewhat distinct from hyperbolic space geodesics. However Berry (2012) notes that the Gutzwiller formula does not imply a relation between the individual energy levels and individual periodic orbits of chaotic systems - that there is a level at each energy for which the action of a periodic orbit is a multiple of Planck, as the number of levels is overestimated. In a billiard, for example, there is an 'infra-red catastrophe', that is, the prediction of levels at arbitrarily low energies. (h) A raw zeta function based on exponentials of the length spectrum. (i) Orbits in a hyperbolic billiard (Sieber & Steiner 1990).

Initially this correspondence between fields caused great excitement in both the mathematics and physics communities, and a number of eminent researchers tried to prove RH, following an unpublished suggestion by Hilbert and Polya that discovering a system of Hermitian matrices whose eigenvalues would be real and might correspond to the zeros of $\xi(s)$ (rotated so the zeros lie on the real line, chosen because it has only the non-trivial zeros)

would thus show they had to be real and hence those of $\zeta(s)$ would be on $x = 1/2$:

$$\zeta\left(\frac{1}{2} + iE_n\right) = 0, \forall n \Rightarrow H|\psi_n\rangle = E_n|\psi_n\rangle \Rightarrow E_n = E_n^*, \forall n.$$

However evidence supporting differences between the Riemann zeta zeros and GUEs comes from careful simulation of the two and studies of the fractal dimension of the graph of zeta zero gaps for large zeros. The matrix size of the GUE is usually taken to be such that the mean eigenvalue spacings for the matrices and for the zeta function zeros at the desired height T

are equal. From fig 1 we have $\frac{T}{2\pi}\left(\log\frac{T}{2\pi} - 1\right) - \frac{7}{8}$, so the mean spacing of the zeros at height

T is $2\pi \log(T / 2\pi)^{-1}$. The mean spacing of the eigenvalues for the GUE is $2\pi / n$, where n is the matrix size. Thus, the statistics of the zeta zeros at height T are to be compared with the random matrix theory for matrices of size $N = \log(T / 2\pi)$.

Comparison shows a Hurst exponent H of 0.095 corresponding to a fractal dimension D of ~ 1.9 (since $D = 2 - H$ in this range) with anti-persistence for zeta, indicating large gaps are followed by smaller ones, self-similarity over a wide range of values and significant differences from corresponding GUE systems. When corresponding block sizes of zeros and random matrices are used, Hurst exponents for the zeros and matrices are 0.34 and 0.65, suggesting fundamental differences in fractal structure (Shanker 2006).

(e) The Search for a Zeta Quantum Operator

The correspondence between the Selberg trace formula

$$\sum_{j=0}^{\infty} h(k_j) = \frac{\mu(D)}{4\pi} \int_{-\infty}^{\infty} kh(k) \tanh(\pi k) dk + \sum_p l_p \sum_{n=1}^{\infty} \frac{g(nl_p)}{2 \sinh(nl_p / 2)}$$

and the prime counting function noted earlier becomes even closer when we consider the form of the Riemann-Weil explicit formula:

$$\sum_{j=0}^{\infty} h(\gamma_j) = \frac{1}{2\pi} \int_{-\infty}^{\infty} h(k) \frac{\Gamma}{\Gamma'}\left(\frac{1}{4} \frac{ik}{2}\right) dk + h\left(\frac{i}{2}\right) + h\left(-\frac{i}{2}\right) - \log \pi g(0) - 2 \sum_p \log p \sum_{n=1}^{\infty} p^{-n/2} g(n \log p)$$

This has suggested to many physicists that a similar treatment could be given to the primes and Riemann's zeta. However the analogy fails in two respects. The $1/2\sinh$ term above only converges to $p^{n/2}$ for large values of p , and the minus sign in the last term is potentially fatal. There are thus major challenges, as we shall see.

In attempting to create a convergence between Hermitian operators and the Riemann zeta function, researchers have constructed a variety of candidates. Berry (1999, Berry & Keating 1999) endeavoured to modify the classical operator $H = xp$, of position and momentum of a particle moving in 1-D, to establish an operator having correspondence with zeta, highlighting several putative connections between this and the zeta zeros. The classical trajectories are $x(t) = x_0 e^{t'}$, $p(t) = p_0 e^{-t'}$, forming unbounded hyperbolae in phase space that would have a continuous spectrum, rather than the discrete spectrum of the zeros.

The space on which this acts is not elucidated and the complex plane would need to be 'sewn up' in Berry's own words into a region that makes the dynamics quantally bound. They thus introduced a minimal length and momentum whose product is the Planck quantum \hbar . The

semiclassical number of states is given by the area below the hyperbola and above the boundaries and is given, in Planck units by $\frac{E}{2\pi} \left(\log \frac{E}{2\pi} - 1 \right) + 1$, which surprisingly coincides with the asymptotic distribution of the zeros in fig 1 if the 7/8 is replaced by 1, which can be resolved if the Maslow phase is -1/8 taking into account the particle travelling in only one quadrant of phase space. However there is no elucidated relationship between the primes and the periodic orbits of the Riemann dynamics.

Connes (1998) made a different regularization of the same operator limiting both x and p to an arbitrary cutoff and afterwards scaling this to infinity, but this does not fully obtain the asymptotic formula for the zeros (Sierra 2008), although it has since been realized experimentally (see below).

The GUE statistics corresponds to random systems where time reversal is broken, which gives a strong indication that the Riemann Hamiltonian H must break this symmetry. Berry noticed the time irreversibility would follow from the analogy between the quantum fluctuation about the average between quantum chaotic systems and the Riemann zeros:

$$N_{osc} = \frac{1}{\pi} \sum_{\gamma} \sum_{m=1}^{\infty} \frac{\sin(mET_{\lambda})}{2m \sinh(m\lambda_{\gamma} / 2)} \leftrightarrow N_{osc} = \frac{-1}{\pi} \sum_p \sum_{m=1}^{\infty} \frac{\sin(mE \log p)}{mp^{m/2}},$$

This likewise suffers from the sign difference previously mentioned. The analogy with quantum chaos led Berry to propose that: (1) The quantum system has a classical counterpart as there is no explicit Planck constant in the right hand formula above, (2) that it lacks time reversal symmetry, (3) is chaotic and unstable and (4) that it is one dimensional, with one expanding dimension due to the $p^{m/2}$ term and no contracting dimensions (Schumayer & Hutchinson 2011). The connection with Quantum Chaos also helped explain some numerical discrepancies found by Odlyzko between random matrix theory and the statistics of zeros for long range spectral correlations, which are due to the shortest periodic orbits, where universality no longer holds.

Connes endeavours to circumvent the sign difference between the logs of the primes and semi-classical orbits by making them an absorption spectrum in the zeta case, rather than the usual 'emission' spectra of Selberg eigenvalues. His operator becomes the Perron-Frobenius transfer operator on an abstract space. The primes acting on the Euler product are built in using a space of p -adic numbers and their units. The proof of the Riemann hypothesis is then transformed into establishing the proof of a certain classical trace formula in abstract space governed by global fields. However there is no evidence of an actual proof of RH in the intervening period (Khalkhali 2005, Connes 2005, Connes, Consani & Marcolli 2007).

The $H = xp$ model can be realized physically (fig 11) in a charged particle moving in a plane under a transverse magnetic field with a saddle-shaped electrostatic potential (Sierra 2008).

The Lagrangian describing the dynamics $L = \frac{\mu}{2}(\dot{x}^2 + \dot{y}^2) - \frac{eB}{c} \dot{y}x - e\lambda xy$ has two normal

modes, with real and imaginary angular frequencies, ω_c cyclotronic and ω_h hyperbolic. In the limit where $\omega_c \gg \omega_h$, only the lowest Landau cyclotronic level applies and we get

$L = p\dot{x} - |\omega_h|xp$. If we put the particle into a box the number of classical states with energy 0

to E becomes $\frac{E}{2\pi} \log \frac{L^2}{2\pi l^2} \frac{E}{2\pi} \left(\log \frac{E}{2\pi} - 1 \right)$ where l is the magnetic length and l is the box size, which coincides with Connes' version of the smooth counting of the Riemann zeros. Sierra and Townsend (2008) speculate that the oscillating terms in the zero distribution might be affected by higher Landau levels.

(d) Quantum Realizations of the Primes and Zeta Function Zeros

Contradicting the notion that the zeta zeros violate time reversal symmetry because they behave like the GUE, Wu and Sprung (1993) generated a one-dimensional, integrable, quantum mechanical model which is invariant under time reversal and yet possess the Riemann zeta zeros as energy eigenvalues, displaying the same level-repulsion as that observed in quantum chaos. Despite being integrable, the new quantum potential was irregular and proved to be multi-fractal in nature (fig 11).

Firstly they derived a smooth semi-classical potential, which generates the smooth part of the zero distribution $N(E) = \frac{I}{h} \iint_{H < E} dx dp = \frac{2}{\pi} \int_0^{x_{\max}} \sqrt{E - V(x)} dx$. Solving, they get an implicit

expression for $V(x)$: $x(V) = \frac{1}{\pi} \left[\sqrt{V - V_0} \ln \left(\frac{V_0}{2\pi} \right) + \sqrt{V} \ln \left(\frac{\sqrt{V} + \sqrt{V - V_0}}{\sqrt{V} - \sqrt{V - V_0}} \right) \right]$, which for suitable V_0

gives $x(V) = \frac{\sqrt{V}}{\pi} \ln \left(\frac{2V}{\pi e^2} \right)$. This it is then modified to model the low-lying zeta zeros exactly,

by setting up a least-squares routine, to minimize the difference between the actual energy eigenvalues and the exact zeros. The potential curve becomes coarse, resembling a random potential. Using fractal box-counting they found a fractal dimension of $d = 1.5$ for the potential reconstructing the Riemann zeta zeros.

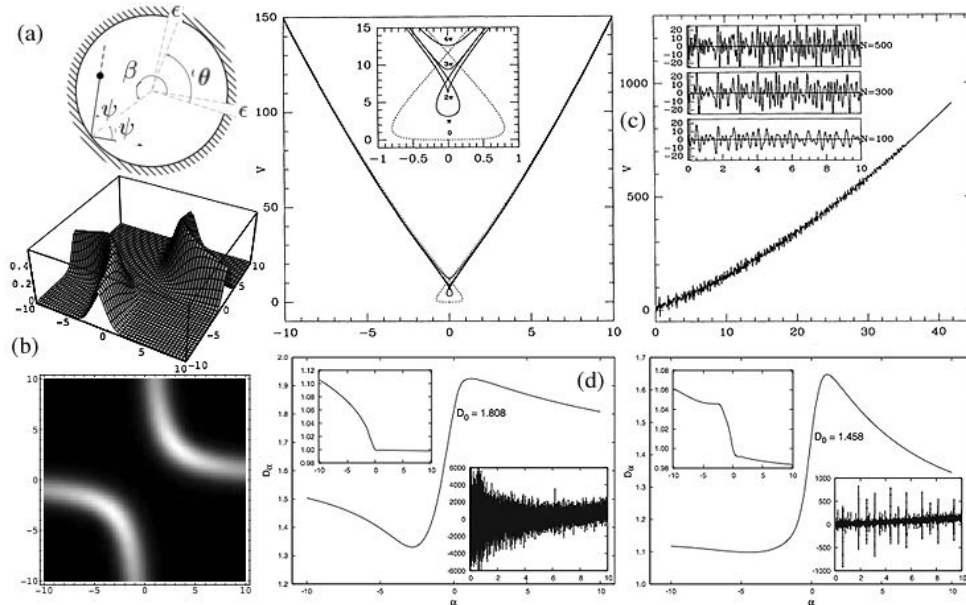


Fig 11: (a) Circular stadium with slits (Bunimovich & Dettmann 2005). (b) Electrostatic potential generating the $H = xp$ experimental system (Sierra & Townsend 2008). (c) Smooth and fractal potentials generating the smoothed and discrete Riemann zeros as spectra (Wu & Sprung 1993). Multifractal spectrum Renyi dimension portraits of the same system (Schumayer et al. 2008).

Schumayer et al. (2008) confirmed these results using the inverse scattering transformation, which guarantees the uniqueness of the potential in one-dimension. They also found the prime numbers can be considered as an energy spectrum, thus a potential can be associated with them which also proves to be fractal, with $d = 1.8$. Thus the two sets of the zeta zeros and prime numbers can be mapped onto each other, but the nearest-neighbour spacing distribution of prime numbers is known to be a Poisson-like (almost uncorrelated random distribution) while that of the Riemann zeros is rooted in the Gaussian Unitary Ensemble, and exhibits the corresponding correlations shown in fig 10. One may, therefore, conclude that Riemann's formulae convert two very different random distributions into each other - the almost uncorrelated sequence of the primes from the interference of the highly-correlated Riemann zeros. Finally they established that both the potentials are multifractal by portraying their Renyi fractal spectra (fig 11).

Julia (1990, 1994) proposed the idea of a non-interacting boson gas, where a single *primon* particle can have discrete 'primal' energy $\varepsilon_0, \varepsilon_1, \varepsilon_2, \dots, \varepsilon_n = \varepsilon_0 \ln(p_n)$. Since the particles are not interacting, a many-body state can be represented by a natural number n with unique factorization, $n = p_1^{m_1} \cdots p_k^{m_k}$ which tells us that m_k particles are in the $|p_k\rangle$ state, $k = 1 - n$.

Hence, each many-body state is enumerated once, so the total energy of the system, in the state $|n\rangle$ is $E_n = \sum_{i=1}^k \varepsilon_0 m_i \ln(p_i) = \varepsilon_0 \ln(p_1^{m_1} \cdots p_k^{m_k}) = \varepsilon_0 \ln(n)$. The partition function from this

spectrum is $Z_B = \sum_{n=1}^{\infty} \exp\left(-\frac{E_n}{k_B T}\right) = \sum_{n=1}^{\infty} \left(\frac{1}{n^s}\right) = \zeta(s)$, where $s = \varepsilon_0 / k_B T$ the root energy times

the inverse temperature. The domain of the zeta function shows that this is well-behaved for $s > 1$, i.e. at low-temperatures, while $s \leq 1$ is physically unacceptable. The boundary, $s = 1$ represents a critical temperature, called the Hagedorn temperature above which the system cannot be heated, since its energy becomes infinite. If we consider fermions rather than bosons, because of the Pauli exclusion principle, m_i can only be 0 or 1 for all i . so the many-body states are labeled by the square-free numbers, sieved from the natural numbers by the Mobius function and we arrive at $Z_B = \zeta(s) / \zeta(2s)$.

Julia claims that the continuation across or around this critical temperature can help understand certain phase transitions in string theory (Deo et al., 1989) and quark confinement. In the Riemann gas, the asymptotic density of states grows exponentially $d(E) = \varepsilon^E$ as in string theory. One can also define a transition between bosons and fermions by introducing an extra parameter, k which defines an imaginary particle, the non-interacting parafermions of order k , 0 to $k - 1$ of which can occupy the same state, with $k = 2$ being normal fermions, and $k \rightarrow \infty$ representing normal bosons, with partition function $Z_B = \zeta(s) / \zeta(ks)$. Using Dirichlet series convolutions, one can extend this model into boson-fermion mixtures in which a unitary twisting function can inter-convert between bosons and fermions. The Mobius function, which is the identity function with respect to convolution (free mixing) reappears in supersymmetric quantum field theories as a possible representation of the $(-1)^F$ operator, where F is the fermion number operator (Schumayer & Hutchinson 2011). This brings us to further work on string theory and zeta.

(e) Superstring Theories and Zeta Functions

String theories can be formulated using the path integrals to compute the scattering amplitudes. The conformal invariance of the string theory forces the amplitude to be invariant under the action of the modular group to the extent that any multi-loop amplitude

in any conformal invariant string theory may be deduced from purely algebraic objects on moduli spaces M_p of Riemann surfaces.

For bosonic strings this permitted the computation of the vacuum to vacuum amplitude up to four loops in terms of modular forms. Computation of g -loop amplitudes in superstring perturbation theory is more complicated because the fermion interactions make the splitting of chiral and anti-chiral modes difficult, requiring the construction of a suitable measure on the super moduli space of genus g super-Riemann surfaces.

The end result is that the study of one, two and three loop superstring theory involves higher order versions of $SL(2, \mathbb{Z})$, in particular automorphic forms of the symplectic group $Sp(2g, \mathbb{Z})$, defined on the genus g Siegel upper space H_g , the set of $g \times g$ symmetric matrices over the complex numbers whose imaginary part is positive definite. A symplectic matrix is a $2g \times 2g$ matrix M with real entries that satisfies the condition $M^T A M = A$, where A is a fixed non-singular anti-symmetric matrix, whose determinants are again 1. The symplectic group governs Hamiltonian systems, since these are preserved by the group operation.

This situation leads to the investigation of superstring theories in terms of modular groups and modular forms, leading to extended treatments expanding the role of Selberg and Riemann zeta functions in higher dimensions, in which Riemannian manifolds are defined as the quotients of $Sp(2g, \mathbb{Z}) \backslash Sp(2g, \mathbb{R})$ in the same manner as previously. This has in turn led to several claims about the Riemann hypothesis.

Cacciatori and Cardella (2010, 2011) examine the equidistribution of long horocycles (curves whose perpendicular geodesics all converge asymptotically in the same direction - see fig 6), which are known to tend to a uniform distribution over $SL(2, \mathbb{Z}) \backslash SL(2, \mathbb{R})$. Zagier (1981) has shown that, in this case, a single $SL(2, \mathbb{Z})$ invariant smooth function of rapid decay as $z \rightarrow i\infty$ would prove RH true if the horocycle convergence rate is $O(F(z))^{3/4}$, $F(z) \rightarrow 0$. In turn, they deduce that certain values of the convergence rates in the genus- g case are compatible only with the Riemann hypothesis. For $g = 1$ uniform distribution can determine constraints on the ultraviolet property of non tachyonic (one-loop) closed string spectra.

In a second paper by a related team, Angelantonj et al. (2011) find that the spectrum of physical excitations in classically stable oriented closed string vacua not only must enjoy asymptotic supersymmetry but at very large mass, bosonic and fermionic states must follow a universal oscillating pattern, whose frequencies are related to the zeros of the Riemann zeta function, with the convergence rate of the overall number of the graded degrees of freedom to the value of the vacuum energy determined by the Riemann hypothesis.

He et al. (2015) note that the crossing symmetrized Veneziano amplitudes of bosonic string theory can likewise be rewritten in terms of ratios of the Riemann zeta function

$$A_4(s, t, u) = \prod_{s, t, u} \frac{\zeta(1 + \alpha(x))}{\zeta(-\alpha(x))}, \alpha = \text{linear Reggae trajectory}, \text{ leading again to claims about RH, but}$$

here the zeta function is simply finessed through a ratio of gamma functions.

These very esoteric abstract representations, leading directly into the putative TOE (theory of everything) of the universe do not prove RH any more than Odlyzko's computed zeros do because they only reflect statistical or experimental approximations. They also raise a

fundamental question that surrounds all the physical attempts to address RH. Do such methods actually help to expose RH to proof, or do they simply become part of a logical regress that originates from the primordial relationship between the natural primes and the integers and between the very concepts of addition and multiplication at the root of number?

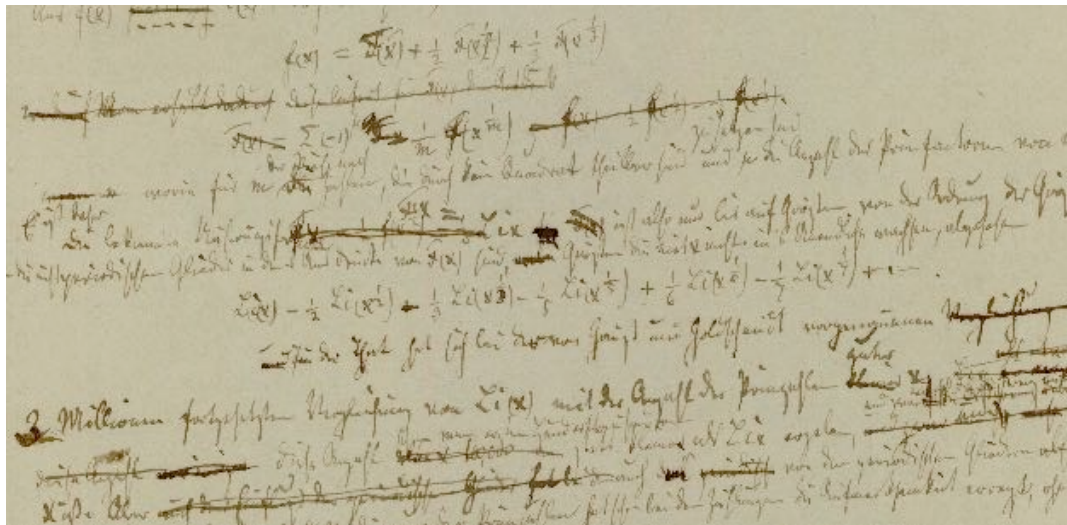


Fig 12: Excerpt from Riemann's original 4-page manuscript.

References

- Angelantonj C, Cardella M, Elitzur S, Rabinovic E (2011) *Vacuum stability, string density of states and the Riemann zeta function* ArXiv 1012.5091.
- Berry, M (1989) Quantum physics on the edge of chaos New Scientist 29 Oct
<http://www.fortunecity.com/emachines/e11/86/edgechaos.html>
- Berry M. (2012) Martin Gutzwiller and his periodic orbits <http://www.sps.ch/en/articles/various-articles/the-legacy-of-martin-gutzwiller/martin-gutzwiller-and-his-periodic-orbits/>
- Berry M, Keating J. (1992) A new approximation for $\zeta(1/2 + it)$ and quantum spectral determinants Proc. Roy. Soc. Lond. A437 151-173.
- Berry M, Keating J (1999) *The Riemann Zeros and Eigenvalue Asymptotics* SIAM Rev. 41/2 236-266.
- Berry M, Keating j (1999) $H = xp$ and the Riemann Zeros
http://www.phy.bris.ac.uk/people/berry_mv/the_papers/Berry306.pdf
- Bian, Ce (2010) *Computing $GL(3)$ automorphic forms* Bull. London Math. Soc. 42 (2010) 827-842.
 Code: <http://www.maths.bris.ac.uk/~macxb/>
- Booker, Andrew (2008) *Uncovering a New L-function* Notices of the American Mathematical Society 55/9 1088-94. <http://www.staff.science.uu.nl/~plaza101/Booker.pdf>
- Borthwick, David (2014) *Distribution of Resonances for Hyperbolic Surfaces* Experimental Mathematics, 23:1, 25-45, doi:10.1080/10586458.2013.857282.
- Bunimovich L & Dettmann C (2005) *Open Circular Billiards and the Riemann Hypothesis* Phys. Rev. Lett. 94/10 100201.
- Cacciatori S, Cardella M (2010) *Equidistribution Rates, Closed String Amplitudes, and the Riemann Hypothesis* ArXiv 1007.3717
- Cacciatori S, Cardella M (2011) *Uniformization, unipotent flows and the Riemann hypothesis* ArXiv 1102.1201
- Casati G, Maspero G, Shepelyanski D (1999) *Quantum Fractal Eigenstates* Physica D 131 311-6.
- Chaudhury S, Smith A, Anderson B, Ghose S, Jessen P (2009) *Quantum signatures of chaos in a kicked top* Nature 461 768-771
- Cogdell J *Lectures on L-functions, Converse Theorems, and Functoriality for GL_n*
<http://www.prime.sdu.edu.cn/cimpaschool/fields.ps>
- Connes, Alain (1996) *Trace Formula in Noncommutative Geometry and the Zeros of the Riemann Zeta Function* C.R. Acad. Sci. Paris 323, 1231-6.
- Connes Alain (2005) *Noncommutative Motives, Thermodynamics, and the Spectral Realization of Zeros of Zeta*
<http://online.itp.ucsb.edu/online/strings05/connes2/rm/jwvideo.html>
- Connes Alain, Marcolli Matilde (2006) *A walk in the noncommutative garden* ArXiv: 0601054

- Connes Alain, Consani Caterina, Marcolli Matilde (2007) *Noncommutative geometry and motives: the thermodynamics of endomotives* ArXiv: 0512138
- Conrey J. Brian (1989) *More than two fifths of the zeros of the Riemann zeta function are on the critical line* J. reine angew. Math 399 1-26.
- Conrey, J. Brian (2003), *The Riemann Hypothesis* Notices of the American Mathematical Society 50/3 341-353, <http://www.ams.org/notices/200303/fea-conrey-web.pdf>.
- Cremona J (1997) *Algorithms for Modular Elliptic Curves* 2nd ed. Online Edition <http://homepages.warwick.ac.uk/~masgaj/book/fulltext/index.html>
- Daney, Charles *The Mathematics of Fermat's Last Theorem* <http://cgd.best.vwh.net/home/flt/flt01.htm>
- Deligne P (1979) *Valeurs de fonctions L et périodes d'intégrales* Proceedings of the Symposium in Pure Mathematics, 33.2, Providence, RI: AMS, pp. 313-346. http://www.ams.org/online_bks/pspum332/pspum332-ptIV-8.pdf
- Deo, N., Jain S, & Tan C (1989) *String distributions above the Hagedorn energy density* Phys. Rev. D 40/8 2626.
- Dokchitser, Tim (2002) *Computing special values of motivic L-functions* <http://arxiv.org/abs/math.NT/0207280> <http://www.dpmms.cam.ac.uk/~td278/computel/> See also: <http://www.sagemath.org/>
- Eckhardt G et al. (1995) *Pinball scattering* in Casati G & Chirikov B eds. *Quantum Chaos* Camb. Univ. Pr. 405.
- Farmer D, Lemurell S *Maass Form L-Functions* http://www.math.chalmers.se/~sj/forskning/level11_2a.pdf
- Farmer D, Ryan N., Schmidt R (2010) *Testing the functional equations of a high-degree Euler product* ArXiv: 1011.1307
- Fraczek, Markus (2012) *Character deformation of the Selberg zeta function for congruence subgroups via the transfer operator* <https://homepages.warwick.ac.uk/staff/M.Fraczek/pdf/fraczek-thesis-2012.pdf>
- Franca G, LeClair A (2014) *A theory for the zeros of Riemann ζ and other L-functions* ArXiv: 1407.4358.
- Franel, J.; Landau, E. (1924), *Les suites de Farey et le problème des nombres premiers*, Göttinger Nachr.: 198-206.
- Gourdon Xavier, Sebah Pascal (2003) *Numerical evaluation of the Riemann Zeta-function* Numbers, constants and computation 1 <http://numbers.computation.free.fr/Constants/Miscellaneous/zetaevaluations.pdf>
- Gutzwiller, M. (1971) *Periodic orbits and classical quantization conditions* J. Math. Phys. 12, 343-358.
- Gutzwiller, Martin (1992) *Quantum Chaos* Scientific American Jan. 266, 78-84.
- Harron R (2010) *Critical integers of motivic L-functions and Hodge numbers* <http://math.bu.edu/people/rharron/research/CriticalIntegers.pdf>
- He Y, Jejjala V, Minic D (2015) *From Veneziano to Riemann: A String Theory Statement of the Riemann Hypothesis* ArXiv 1501.0197
- Hilgert J, Mayer D (2004) *The dynamical zeta function and transfer operator for the Kac-Baker model* Contemporary Mathematics 364 67-92. arXiv 0111063.
- Ingham, Albert E. (1932, rep 1990), *The Distribution of Prime Numbers*, Cambridge University Press, MR1074573, ISBN 978-0-521-39789-6.
- Julia, B. (1990) in *Number Theory and Physics* (ed) M. Luck, P. Moussa (Springer, Berlin) 276.
- Julia, B. (1994) *Thermodynamic limit in number theory: Riemann-Beurling gases* Physica A 203(3-4) 425.
- Keating J, Sieber M (1994) *Calculation of Spectral Determinants* Proc. Royal Soc. A 447/1930 413-437.
- Khalkhali M (2005) *What is new with Connes' approach to the Riemann hypothesis?* <http://www-home.math.uwo.ca/~masoud/files/TehProg.pdf>
- King, Chris C. (2009) *Exploring Quantum and Classical Chaos in the Stadium Billiard* 2013 Quanta 3/1 16-31 doi: 10.12743/quanta.v3i1.23 <http://dhushara.com/DarkHeart/QStad/QStad.pdf>
- King, Chris C. (2009) *Riemann Zeta Viewer* <http://www.dhushara.com/DarkHeart/RZV/RZViewer.htm>
- King, Chris C. (2011) *A Dynamical Key to the Riemann Hypothesis* <http://dhushara.com/DarkHeart/key/key2.htm>
- Kotnik, Tadej; te Riele, Herman (2006) *The Mertens Conjecture Revisited* In Hess, Florian. *Algorithmic number theory*. Proceedings. Lecture Notes in Computer Science. Berlin: Springer-Verlag. pp. 156-167.
- LeClair A (2013) *An electrostatic depiction of the validity of the Riemann Hypothesis and a formula for the N-th zero at large N* ArXiv: 1305.2613
- Liu B, Zhang G, Dai J Zhang H (1998) *Eigenvalues and Eigenfunctions of a Stadium-Shaped Quantum Dot Subjected to a Perpendicular Magnetic Field* Chin. Phys. Lett. 15/9 628.
- Lozano-Robledo, Álvaro (2009) *Elliptic Curves, Modular Forms and their L-functions* Student Mathematical Library Ias/Park City Mathematical Subseries, Volume: 58 <http://www.dhushara.com/DarkHeart/key/ellipticM.pdf> Password="ellipticM"
- Maldacena J (1998) *The Large N Limit of Superconformal Field Theories and Supergravity* Adv. Theor. Math. Phys 2: 231-252. arXiv:hep-th/9711200.
- Maldacena J, Susskind L (2013) *Cool horizons for entangled black holes* Fortschr. Phys. 61/9, 781-811 doi:10.1002/prop.201300020.
- Marklof J (2008) *Selberg's Trace Formula: An Introduction* <http://www.maths.bris.ac.uk/~majm/bib/selberg.pdf>

- Matthies C, Steiner F (1991) *Selberg's ζ function and the quantization of chaos* Physical Rev. A 44/12 R7877-80.
- Mayer, Dieter (1991) *The thermodynamic formalism approach to Selberg's zeta function for $PSL(2, \mathbb{Z})$* , Bull. Amer. Math. Soc. (N.S.) 25/1, 55-60.
- Montgomery H, (1973) *The pair correlation of zeros of the zeta function* in Analytic Number Theory 24 AMS Proc. Symposia in Pure Maths 181.
- Moore F, Robinson J, Bharucha C, Sundaram B, Raizen M, (1995) *Atom optics realization of the quantum δ -kicked rotor* Physical Review Letters 75/25 4598-4601.
- Odlyzko, Andrew (2001) *The 10²²-nd zero of the Riemann zeta function*, in *Dynamical, Spectral, and Arithmetic Zeta Functions*, M. van Frankenhuysen and M. L. Lapidus, eds., Amer. Math. Soc., Contemporary Math. series 290 139-144. <http://www.dtc.umn.edu/~odlyzko/doc/zeta.10to22.pdf>
- Odlyzko, A., te Riele, H. (1985) *Disproof of the Mertens conjecture*, Journal für die reine und angewandte Mathematik 357: 138-160.
- Oort, Franz (2014) *The Weil Conjectures* NAW 5/15 nr. 3 211
<http://www.nieuwarchief.nl/serie5/pdf/naw5-2014-15-3-211.pdf>
- Patterson S, Perry P (2000) *The divisor of Selberg's zeta function for Kleinian groups*
<http://www.ms.uky.edu/~math/MAREport/PDF/00-10.pdf>
- Pollicott Mark (2013) *Dynamical Systems and the Ruelle zeta functions*
<https://homepages.warwick.ac.uk/~masdbl/grenoble-16july.pdf>
- Raizen M, Moore F, Robinson J, Bharucha C and Sundaram B (1996) *An experimental realization of the quantum δ -kicked rotor* Quantum Semiclass. Opt. 8 687-692.
- Riemann, Bernhard (1859) <http://www.claymath.org/sites/default/files/riemann1859.pdf>
- Ruelle, David, (2002) *Dynamical zeta functions and transfer operators* <http://preprints.ihes.fr/M02/M02-66.pdf>
- Schumayer D & Hutchinson A (2011) *Physics of the Riemann Hypothesis* ArXiv: 1101.3106.
- Schumayer, D., van Zyl B, Hutchinson D (2008) *Quantum mechanical potentials related to the prime numbers and Riemann zeros* Phys. Rev. E 78/5 056215.
- Shanker O (2006) *Random matrices, generalized zeta functions and self-similarity of zero distributions* J. Phys. A 39/45 13983.
- Sieber M & Steiner F (1990) *Classical And Quantum Mechanics Of A Strongly Chaotic Billiard System* Physica D 44 248-266.
- Sieber M & Steiner F (1991) *Quantization of Chaos* Physical Review Letters 67/15 1941-4.
- Sierra G (2008) *A physics pathway to the Riemann hypothesis* ArXiv: 1012.4264
- Sierra G & Townsend P (2008) *Landau levels and Riemann zeros* ArXiv: 0805.4079
- Silverman J.H. (1986) *The Arithmetic of Elliptic Curves*, Springer-Verlag.
- Skewes, S. (1933), *On the difference $\pi(x) - li(x)$* J. Lond. Math. Soc. 8 277-283.
- Skewes, S. (1955), *On the difference $\pi(x) - li(x)$ (II)* Proc. Lond. Math. Soc 5 48-70.
- Steck D (2009) *Passage through chaos* Nature 461 736-7.
- Stein W. (2007) *Modular forms, a computational approach*, (appendix P. E. Gunnells), Grad. Studies in Math., vol. 79, Amer. Math. Soc., Providence, RI.
<http://modular.math.washington.edu/books/modform/modform/index.html>
- Stein W. (2008) *An introduction to computing modular forms using modular symbols* Algorithmic Number Theory MSRI Publications 44 <http://www.math.leidenuniv.nl/~psh/ANTproc/20stein.pdf>
- Strömberg, Fredrik (2008) *Computation of selberg zeta functions on hecke triangle groups* arXiv 0804.4837
- Titchmarsh, E. C. (1986) *The Theory of the Riemann zeta-function*, 2nd edition, The Clarendon Press, Oxford Univ. Press, New York Ch X, 10.25
- Tresp C (2011) *Semiclassical Quantization of Chaotic Systems II - Gutzwiller's Trace Formula* http://itp1.uni-stuttgart.de/lehre/vorlesungen/hauptseminar/ss2011/3_Vortrag_Tresp.pdf
- Weiss, C., Page, S Holthaus M (2004) *Factorising numbers with a Bose-Einstein condensate* Physica A 341 586.
- Wiles, Andrew (1995), *Modular elliptic curves and Fermat's last theorem*, Annals of Mathematics. Second Series 141 (3): 443-551.
- Williams F (2003) *A zeta function for the BTZ black hole* Internat. J. Modern Phys. A 18/12 2205-2209.
- Williams F (2010) *The role of the Patterson-Selberg zeta function of a hyperbolic cylinder in three-dimensional gravity with a negative cosmological constant* A Window Into Zeta and Modular Physics MSRI Publications 57 329-351.
- Wu H & Sprung D (1993) *Riemann zeros and a fractal potential* Phys. Rev. E 48/4 2595.
- Zagier D (1981) *Eisenstein Series and the Riemann zeta function*, Automorphic Forms, Representation Theory and Arithmetic, Studies in Math. 10, T.I.F.R. Bombay 275-301
<http://people.mpim-bonn.mpg.de/zagier/files/scanned/EisensteinRiemannZeta/fulltext.pdf>
- Zagier, Don *New points of view on the selberg zeta function*
<http://people.mpim-bonn.mpg.de/zagier/files/tex/NewPointsSelbergZeta/fulltext.pdf>

Appendix 1: MuPad Code for the Selberg Zeta Function of Hecke Triangle Groups

This code will run as is in Matlab using the commands `read(symengine, 'SelbergZHecSZH.mu')` and `t=feval(symengine, 'SelbergZ', 3, s, 50, 1e-6)`; if saved into the file 'SZH.mu'. A single value takes about 30 mins to compute.

```
//MuPAD-SESSION
/* Algorithms for computing the Selberg Z-function for Hecke Triangle Groups
Author: Fredrik Strömberg 04 March 2008.
Copyright:      This file is distributed under the GNU GPL v2. */

/* Some global parameters : */
is_set:=FALSE: /* is set to true if we have set all parameters */
MAXIT:=10000: /* maximum number of iterations for various loops */
DIGITS:=30: /* Good starting number of digits */
q_set:=3:

/* Pochhammer symbol */
pochhammer:=
proc(z,n)
    local j;
begin;
    poc:=1:
    for j from 0 to n-1 do:
        poc:=poc*(z+j):
    end_for:
    poc:
end_proc:

/* Setup the matrix Nij of indices in the transfer operator */
setup_trop:=
proc(qin)
    local i,j,q;
begin;
    if(is_set and (q_set=qin)) then:
        return:
    end_if:
    q:=qin:
    lambda:=float(2*cos(PI/q)):
    dim:=0:
    delete NIJ:
    if(q mod 2 = 0) then
        R:=1:
        h:=(q-2)/2:
        dim:=2*h:
        NIJ:=matrix(dim,dim):
        NIJ[1,h]:=2:
        for i from 2 to h do:
            NIJ[i,i-1]:=1:
            NIJ[i,h]:=2:
        end_for:
        for i from h+1 to 2*h-1 do:
            NIJ[i,h]:=1:
        end_for:
        NIJ[2*h,h]:=1:
        for j from 1 to dim do:
            for i from 1 to h do:
                NIJ[j,dim+1-i]:=-NIJ[dim+1-j,i]
            end_for:
        end_for
    elif(q=3) then:
        R:=(sqrt(5)-1)/2:
        dim:=2:
        h:=0:
        NIJ:=matrix([[3,-2],[2,-3]]):
    elif(q>=5) then:
        R:=lambda/2-1+1/2*sqrt((2-lambda)^2+4):
        h:=(q-3)/2:
        dim:=4*h+2:
```

```

NIJ:=matrix(dim,dim):
NIJ[1,2*h]:=2:
NIJ[1,2*h+1]:=3:
NIJ[2,2*h+1]:=2:
for i from 3 to 2*h+1 do:
    NIJ[i,i-2]:=1:
    NIJ[i,2*h+1]:=2:
end_for:
for i from 2*h+2 to 4*h do:
    NIJ[i,2*h]:=1:
    NIJ[i,2*h+1]:=2:
end_for:
for i from 4*h+1 to 4*h+2 do:
    NIJ[i,2*h]:=1:
    NIJ[i,2*h+1]:=2:
end_for:
for j from 1 to dim do:
    for i from 1 to 2*h+1 do:
        NIJ[j,dim+1-i]:=-NIJ[dim+1-j,i]:
    end_for:
end_for:
end_if:
R:=float(R):
q_set=q:
is_set:=TRUE:
end_proc:

/* We can now compute the matrix approximation of level N, ANN of the
transfer operator for the matrix NIJ*/
ANN:=
proc(q,s,M)
    local l,n,i,j,k,lambda,B;
begin;
    if((is_set=FALSE) or (q<>q_set)) then:
        setup_trop(q):
    end_if:
    lambda:=float(2*cos(PI/q)):
    A:=matrix(dim*(M+1),dim*(M+1));
    for l from 0 to 2*M do:
        Z[l]:=zeta(2*s+1)
    end_for:
    for n from 0 to M do:
        fn:=1/n!*lambda^(-n-2*s):
        for k from 0 to M do:
            poc:=pochhammer(2*s+k,n)*fn*lambda^(-k):
            for i from 0 to dim-1 do:
                for j from 0 to dim-1 do:
                    nn:=i*(M+1)+n+1:
                    ll:=j*(M+1)+k+1:
                    B:=NIJ[i+1,j+1]:
                    if(j < dim/2-1 or j > dim/2+1-1 ) then
                        if(B=0) then
                            AA:=0:
                        else
                            AA:=abs(B)^(-2*s-k-n)*sign(-B)^(n+k):
                        end_if:
                    else
                        AA:=Z[k+n]:
                        for l from 1 to abs(B)-1 do:
                            AA:=AA-l^(-2*s-k-n):
                        end_for:
                        AA:=AA*sign(-B)^(n+k):
                    end_if:
                    A[i*(M+1)+n+1,j*(M+1)+k+1]:=poc*AA:
                end_for:
            end_for:
        end_for:
    end_for:
    A:
end_proc:

```



```

/* And to compute the Selberg zeta function we also need det(1-K) */
detlmK:=
proc(q,s)
  local err,tol;
begin;
  if((is_set=FALSE) or q_set<>q)then:
    setup_trop(q):
  end_if:
  tol:=10^(1-DIGITS):
  K:=1:
  if(q=3) then:
    L:=4-R:
  elif(q=4) then:
    L:=sqrt(2.0)+1.0:
  elif(q mod 2 = 0) then:
    L:=(2+lambda)/sqrt(4-lambda^2):
  else:
    L:=(2+R*lambda)/(2-lambda):
  end_if:
  L:=float(L):
  /* print("L=",L):
  for n from 0 to MAXIT do:
  /* l[n]:=(2+lambda*R)^(-2*s-2*n):*/
  l[n]:=L^(-2*s-2*n):
  K:=K*(1-l[n]):
  if(n>1) then
    err:=max(abs(l[n]),abs(l[n-1]))*abs(K):
    if(err<tol) then
      break:
    end_if:
  end_if:
end_for:
K:
end_proc:

SelbergZ:=
proc(q,s,N0,tol)
  local j,k,M,M00,eps,l,DIG1;
begin;
  /* tol:=10^(1-DIGITS):
  l:=3:
  DIG1:=DIGITS:
  err_old:=0:
  M00:=N0:
  for M from N0 to 50 step 10 do:
    err:=1:
    truev:=0:
    A1:=ANN(q,s,M):
    ev1:=sort(numeric::eigenvalues(A1),(x,y)->abs(y)<abs(x));
    A2:=ANN(q,s,M+1):
    ev2:=sort(numeric::eigenvalues(A2),(x,y)->abs(y)<abs(x));
    /* We compare the largest (in magnitude) eigenvalues since the small ones are giving 1
    any way) */
    for k from 1 to nops(ev2) do:
      used[k]:=0:
    end_for:
    for j from 1 to nops(ev1) do:
      for k from 1 to nops(ev2) do:
        if(used[k]=0) then:
          eps:=abs(ev1[j]-ev2[k])/(abs(ev1[j])+abs(ev2[k])):
          if(eps<tol) then:
            end_if:
            if(eps < tol) then:
              truev:=truev+1:
              tv[truev]:=ev2[k]:
              used[k]:=1:
              break:
            end_if:
          end_if:
        end_for:
      end_for:
    end_for:
  end_for:

```

```

    tmp:=1:
    if(truev>0) then:
        err:=abs(tv[truev]):
    end_if:
    if(M>M00+10 or (err>10*err_old)) then:
        /* We also increase the precision */
        M00:=M:
        DIGITS:=DIGITS+20:
    end_if:
    if((truev>0) and (err<tol)) then:
        break;
    end_if:
    err_old:=err:
end_for:
for j from 1 to truev do:
    tmp:=tmp*(1-tv[j]):
end_for:
k:=detlmK(q,s):
DIGITS:=DIG1:
[tmp/k,abs(tv[truev]),M]:
end_proc:

/* The "rotated" real valued Z */
/* The third argument should be a previously calculated function value, */
/* used to determine which branch to use. Otherwise the default is 1 */

/* Scattering matrix phi_q(s) for Hecke triangle group G_q */
PhiQ:=
proc(q,s,N0,tol)
    local M;
begin;
    p:=float(PSI(s,q)):
    z1:=SelbergZ(q,s,N0,tol):
    M:=z1[3]:
    z2:=SelbergZ(q,1.0-s,M,tol):
    print("s=",s):
    rh:=z2[1]/z1[1]/p:
end_proc:

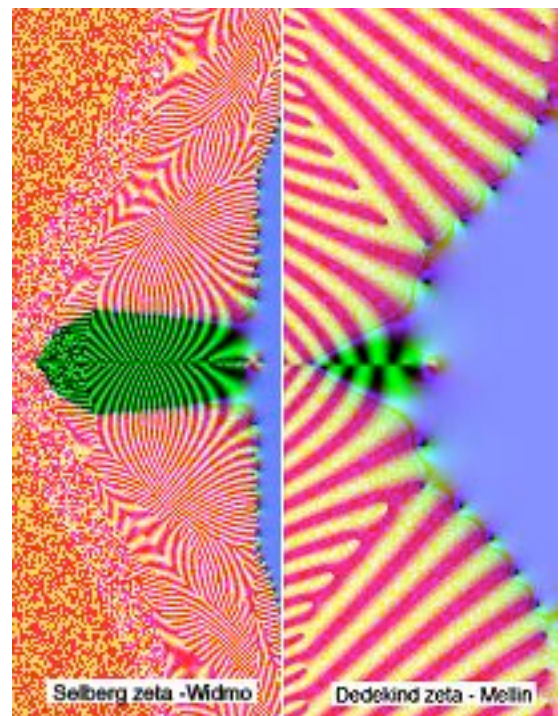
```

Fig 13: Breakdown profiles with increasing real and imaginary values for the transfer operator algorithm and Mellin transform.

Appendix 2: Analytic continuation for Dirichlet series based zeta and L -functions

The following gives a summary of the analytic continuations and Mellin integral transforms for Riemann zeta, Dirichlet L -functions, Dedekind zeta, Hecke L -functions on Gaussian integers, and for the L -functions of elliptic curves and modular forms.

In the generation of these zeta and L -functions, I have used three processes in the open source Mac application RZViewer (King 2009b). In the right half-plane, the Dirichlet series is used. In the left-half plane this is transformed via the appropriate functional equation as listed below. In the central region because the function will begin to have bad approximations towards the critical strip, the Mellin transform formulae, which form the central bridge defining the functional equation are applied.



Tim Dokchitser's computel algorithm, discussed below applies a high-fidelity Mellin transform technique which gives good approximation for a considerably larger region of the complex plane than elementary Mellin transform methods.

Alternatively the Riemann-Siegel formula which has been applied in fast calculation of zeros of the Riemann zeta function (Odlyzko 2001, Gourdon & Sebah 2003) can be used in ways which generalize to other zeta and L -functions.

Riemann zeta

$$\zeta(s) = \pi^{s/2} / \Gamma\left(\frac{s}{2}\right) \int_0^\infty y^{s/2} (\theta(iy) - 1) \frac{dy}{2y}, \phi(t) = e^{-\pi t^2}, \theta(iy) = \sum_{n \in \mathbb{Z}} \phi(ny) = \sum_{n \in \mathbb{Z}} e^{-\pi n^2 y}, \theta(iy) = \frac{1}{\sqrt{y}} \theta\left(\frac{i}{y}\right)$$

$$\pi^{-s/2} \Gamma\left(\frac{s}{2}\right) \zeta(s) = \int_1^\infty (y^{s/2} - y^{(1-s)/2}) (\theta(iy) - 1) \frac{dy}{2y} + \frac{1}{2} \left(\frac{1}{s-1} - \frac{1}{s} \right) = \pi^{-(1-s)/2} \Gamma\left(\frac{1-s}{2}\right) \zeta(1-s)$$

Dirichlet L -functions

$$L(s, \chi) = \pi^{(s+a)/2} / \Gamma\left(\frac{s+a}{2}\right) \int_0^\infty y^{s/2} \theta_\chi(iy) \frac{dy}{2y}$$

$$= \pi^{(s+a)/2} / \Gamma\left(\frac{s+a}{2}\right) \left(\int_{1/N}^\infty y^{s/2} \theta_\chi(iy) \frac{dy}{2y} + \frac{-i^a N^{1-s}}{\langle \bar{\chi}, \varphi \rangle} \int_{1/N}^\infty y^{(1-s)/2} \theta_{\bar{\chi}}(iy) \frac{dy}{2y} \right), \langle \chi, \varphi \rangle = \sum_{n=1}^N \chi(n) e^{2\pi n i / N}$$

$$\text{where } \theta_\chi(iy) = \begin{cases} \sum_{n=1}^\infty \chi(n) e^{-\pi n^2 y}, & a=0 \\ \sum_{n=1}^\infty \chi(n) n y^{1/2} e^{-\pi n^2 y}, & a=1 \end{cases}, \varepsilon(\chi) = \frac{\sqrt{N}}{\sum_{n=1}^N \bar{\chi}(n) e^{2\pi n i / N}}, \theta_\chi(iy) = \frac{-i \langle \chi, \varphi \rangle}{N \sqrt{y}} \theta_{\bar{\chi}}\left(\frac{i}{N^2 y}\right)$$

$$N^{s/2} \pi^{-(s+a)/2} \Gamma\left(\frac{s+a}{2}\right) L(s, \chi) = \int_{1/N}^\infty (Ny)^{s/2} \theta_\chi(iy) \frac{dy}{2y} + \varepsilon(\chi) \int_{1/N}^\infty (Ny)^{(1-s)/2} \theta_{\bar{\chi}}(iy) \frac{dy}{2y}$$

$$= \varepsilon(\chi) \int_{1/N}^\infty \varepsilon(\bar{\chi}) (Ny)^{s/2} \theta_\chi(iy) \frac{dy}{2y} + \int_{1/N}^\infty (Ny)^{(1-s)/2} \theta_{\bar{\chi}}(iy) \frac{dy}{2y} = N^{(1-s)/2} \pi^{-((1-s)+a)/2} \Gamma\left(\frac{(1-s)+a}{2}\right) L(1-s, \bar{\chi})$$

Dedekind zeta

$$\zeta_\circ(s) = \frac{1}{4} \sum_{m, n \text{ not both } 0} \frac{1}{(m^2 + n^2)^s} = \pi^s / \Gamma(s) \int_0^\infty y^s (\theta(iy) - 1) \frac{dy}{4y}, \theta(iy) = \sum_{m, n \in \mathbb{Z}} e^{-\pi(m^2 + n^2)y}, \theta(iy) = \frac{1}{y} \theta\left(\frac{i}{y}\right)$$

$$\pi^{-s} \Gamma(s) \zeta_\circ(s) = \int_1^\infty (y^s + y^{1-s}) (\theta(iy) - 1) \frac{dy}{4y} + \frac{1}{4} \left(\frac{1}{s-1} - \frac{1}{s} \right) = \pi^{-(1-s)} \Gamma(1-s) \zeta_\circ(1-s)$$

Hecke L -functions

$$L(s, k) = \pi^{(s+|k|)} / \Gamma(s+|k|) \int_1^\infty (y^s + y^{1-s}) \theta_\chi(iy) \frac{dy}{4y}, \theta_\chi(iy) = \frac{(-1)^{|k|}}{y} \theta_\chi\left(\frac{i}{y}\right)$$

$$\theta_\chi(iy) = \sum_{m, n \in \mathbb{Z}} (m + ni)^{2k} y^{|k|} e^{-\pi(m^2 + n^2)y} = y^{|k|} \sum_{m=0}^\infty \sum_{n=0}^\infty \text{Re}((m + ni)^{2k}) e^{-\pi(m^2 + n^2)y}$$

$$\pi^{-(s+|k|)} \Gamma(s+|k|) L(s, k) = \int_1^\infty (y^s + y^{1-s}) \theta_\chi(iy) \frac{dy}{4y} = (-1)^{|k|} \pi^{-((1-s)+|k|)} \Gamma((1-s)+|k|) L(1-s, k)$$

Modular forms and elliptic curves

$$\begin{aligned}
 f(q) &= \sum_{n=1}^{\infty} a_n q^n = \sum_{n=1}^{\infty} a_n e^{2\pi i n z} \in S_k(\Gamma_1(N)), \text{ By modularity } f\left(-\frac{1}{Nz}\right) = CN^{-k/2}(-Nz)^k f(z) \\
 \int_0^{i\infty} f(z) z^s \frac{dz}{z} &= \int_0^{i\infty} \sum_{n=1}^{\infty} a_n e^{2\pi i n z} z^s \frac{dz}{z} = \int_0^{i\infty} \theta(z) z^s \frac{dz}{z} = \sum_{n=1}^{\infty} a_n \int_0^{i\infty} z^s e^{2\pi i n z} \frac{dz}{z} \\
 [\text{ where } t &= -2\pi i n z, \phi(t) = e^{-2\pi i t}, \theta(z) = \sum_{n=1}^{\infty} a_n \phi(iz)] \\
 &= \sum_{n=1}^{\infty} a_n \left(\frac{-1}{2\pi n}\right)^s \int_0^{\infty} e^{-t} t^s \frac{dt}{t} = (-2\pi i)^{-s} \Gamma(s) \sum_{n=1}^{\infty} \frac{a_n}{n^s} = (-2\pi i)^{-s} \Gamma(s) L(f, s) = (2\pi)^{-s} \Gamma(s) L(f, s) \\
 \int_0^{i\infty} f(z) z^s \frac{dz}{z} &= \int_0^{i/\sqrt{N}} f(z) z^s \frac{dz}{z} + \int_{i/\sqrt{N}}^{i\infty} f(z) z^s \frac{dz}{z} = \int_{i/\sqrt{N}}^{i\infty} \left(f(z) z^s + i^k CN^{-k/2} f(z) \left(-\frac{1}{Nz}\right)^{s-k} \right) \frac{dz}{z} \\
 &= \int_{1/\sqrt{N}}^{\infty} \left(i^s f(iy) y^s + i^k CN^{-k/2} f(iy) \left(-\frac{1}{Niy}\right)^{s-k} \right) \frac{dy}{y} = \int_{1/\sqrt{N}}^{\infty} \left(i^s y^s + i^k CN^{-k/2} i^{s-k} N^{k-s} y^{k-s} \right) f(iy) \frac{dy}{y} \\
 &= i^s \int_{1/\sqrt{N}}^{\infty} \left(y^s + CN^{k/2-s} y^{k-s} \right) f(iy) \frac{dy}{y} = i^s \int_{1/\sqrt{N}}^{\infty} \left(y^s + CN^{k/2-s} y^{k-s} \right) \sum_{n=1}^{\infty} a_n e^{-2\pi n y} \frac{dy}{y} \\
 L(f, s) &= (2\pi)^s / \Gamma(s) \int_{1/\sqrt{N}}^{\infty} \left(y^s + CN^{k/2-s} y^{k-s} \right) \sum_{n=1}^{\infty} a_n e^{-2\pi n y} \frac{dy}{y} \\
 \Lambda(f, s) &= N^{s/2} (2\pi)^{-s} \Gamma(s) L(f, s), \Lambda(f, s) = i^k w \Lambda(f, k-s), w = \pm 1
 \end{aligned}$$

The analytic continuation of each class of motivic L -function is achieved by applying a product of gamma functions $\gamma(s) = \Gamma\left(\frac{s + \lambda_1}{2}\right), \dots, \Gamma\left(\frac{s + \lambda_d}{2}\right)$ derived from the symmetries in

the θ functions, each of which is generated as $\theta(t) = \sum_{n=1}^{\infty} a_n \phi\left(\frac{nt}{A}\right)$, where $L(s) = \sum_{n=1}^{\infty} a_n n^{-s}$. For each of the cases outlined above, ϕ has a known exponential form and other cases include Bessel functions and more general harmonic exponentials. Because we can express the complete gamma factor as a Mellin transform: $\gamma(s) = \int_0^{\infty} \phi(t) t^s \frac{dt}{t}$, and the L -function is a

Mellin transform of theta:

$$\int_0^{\infty} \theta(t) t^s \frac{dt}{t} = \sum_{n=1}^{\infty} a_n \int_0^{\infty} \phi\left(\frac{nt}{A}\right) t^s \frac{dt}{t} = \sum_{n=1}^{\infty} a_n \int_0^{\infty} \phi(t) \left(\frac{At}{n}\right)^s \frac{dt}{t} = A^s \gamma(s) \sum_{n=1}^{\infty} a_n n^{-s} = A^s \gamma(s) L(s), A = N^{1/2} \pi^{-d/2}$$

we can thus reverse the process of defining the gamma factors through the Mellin transforms and derive the Mellin transform of any L -function by specifying its gamma factors and

generating $\phi(t)$ as the inverse Mellin transform of $\gamma(s)$: $\phi(t) = \int_{c-i\infty}^{c+i\infty} \gamma(s) t^{-s} ds$ to get θ . This

integral can easily be performed numerically on an interval up the critical strip giving good correspondence with known $\phi(t)$. Note that this behaves in the manner of a Fourier

transform on $\gamma(s)$, as t^{-s} is sinusoidal on the imaginary dimension. The functional equations

are derived, in turn, from θ symmetries such as $\theta(t) = \varepsilon t^w \theta(1/t) - \sum_j r_j t^{p_j}$ where p_j are any

pole singularities. For example, for $\zeta(s)$ by Poisson summation $\sum_{n \in \mathbb{Z}} f(n) = \sum_{n \in \mathbb{Z}} \hat{f}(k)$, $\hat{f} = F(f)$, equating the function sum to its summed Fourier transforms, we have $\theta(1/t) = \theta(t) + t + 1$, since the Fourier transform of e^{-nx^2} is $\sqrt{\frac{\pi}{n}} e^{-\pi^2 k^2 / n}$ and $\pi^{-s/2} \Gamma\left(\frac{s}{2}\right) \zeta(s)$ has residues 1, -1 at 0, 1.

A similar result holds for modular forms by modularity, as shown above. We can then evaluate the L -function using θ :

$$A^s \gamma(s) L(s) = \int_1^\infty \theta(t) (t^s + \varepsilon t^{w-s}) \frac{dt}{t} + \sum_j \frac{r_j}{p_j - s}, \text{ since}$$

$$\int_0^1 \theta(t) t^s \frac{dt}{t} = \int_1^\infty \theta(1/t) t^{-s} \frac{dt}{t} = \int_1^\infty \varepsilon t^w \theta(t) t^{-s} \frac{dt}{t} + \sum_j \frac{r_j}{p_j - s}.$$

Hence we have the functional equation: $L^*(s) = \varepsilon L^*(w - s)$.

The computel method is summarized as follows. The method uses the inverse Mellin transform to find $\phi(t)$ and its and its generalization to the incomplete Mellin transform

$G_s(t) = t^{-s} \int_t^\infty \phi(x) x^s \frac{dx}{x}$ based on the residues of the poles of the combined gamma factors and any other poles of L^* . Three separate methods, a Taylor formula for small t , an approximant for mid-range t , and an asymptotic formula for large t , involving continued fraction iterations, are then used to calculate $\phi(t)$, and G_s , to calculate L and its derivatives

using $L^*(s) = \sum_{n=1}^\infty a_n G_s\left(\frac{n}{A}\right) + \varepsilon \sum_{n=1}^\infty a_n G_{w-s}\left(\frac{n}{A}\right) + \sum_j \frac{r_j}{p_j - s}$ and equivalent derivative formulas by differentiating G_s .

Appendix 3 Weil Zeta Function

For every prime power $q = p^n$ there exists, up to an isomorphism, exactly one field K with q elements; this field we denote by $K = \mathbb{F}_q$. Note that $\mathbb{F}_p = \mathbb{Z} / p$, however this is not true for prime powers q . An elliptic curve E over a field K is a non-singular algebraic curve $E \subset \mathbb{P}_{2^k}$ given by a cubic equation having at least one K -rational point.

Consider $y^2 - y = x^3 - x^2$, $x, y \in \mathbb{F}_{2^m}$. This has 4 solutions $x = 0, 1$ $y = 0, 1$ for $m = 1$, since $+1 = -1$ in \mathbb{F}_2 (Oort 2014). We now embed this in the projective plane by $(x, y) = [x:y:1]$, we have $D: y^2 z - y z^2 = x^3 - x^2 z$. Adding the point at infinity $[0:1:0]$ on the line $x = 0$, we get a fifth solution, so $\# D(\mathbb{F}_2) = 5$.

We define $\zeta(s) = \prod_M \frac{1}{(1 - \#(R/M))^{-s}}$, in the same manner as the Riemann zeta function,

where M is a maximal ideal in an algebra R , whose residue class ring R/M is a finite field. For $R = \mathbb{Z}$, any maximal ideal is a prime, so we simply get the Euler product of the Riemann zeta function. One can also apply the definition to polynomial rings $R = \mathbb{Z}[T]$, or $\mathbb{F}_p[T]$ to obtain a new kind of zeta function.

For an elliptic curve, it has been proven by Hasse and more egenerally by Weil that the Hasse-Weil zeta function $Z(T) = \exp\left(\sum_{m=1}^{\infty} \frac{N_m}{m} T^m\right) = \frac{(1-\alpha T)(1-\beta T)}{(1-T)(1-qT)}$, $|\alpha| = |\beta| = \sqrt{q}$. The

substitution $T = q^{-s}$ gives $\zeta(s) = \frac{(1-\alpha q^{-s})(1-\beta q^{-s})}{(1-q^{-s})(1-qq^{-s})}$ with an analytic continuation, since

$\alpha \leftrightarrow q/\alpha$ now gives the functional equation $s \leftrightarrow 1-s$, which has zeros on the critical line $x = 1/2$ since

$$1 - \alpha q^{-s} = 0 \Leftrightarrow e^{-s \ln q} = \alpha^{-1} \Leftrightarrow e^{-(a+ib) \ln q} = \alpha^{-1} \Rightarrow |e^{-(a+ib) \ln q}| = q^{-a} = |\alpha^{-1}| = 1/\sqrt{q} \Rightarrow a = 1/2!$$

If we take the logarithmic derivative $\frac{TZ'(T)}{Z(T)} = \sum_{m>0} N_m T^m$, it follows that

$$N_m(E/F_q) = \#E(F_{q^m}) = 1 - (\alpha^m + \beta^m) + q^m.$$

The zeta function can be generalized to a genus- g curve, embedded in an Abelian variety where the numerator then consists of a product of $2g$ terms $(1 - a_i T)$.

For F_2 , we have $\#D(F_2) = 5 = 1 - (\alpha + \beta) + 2$, so we have $\alpha + \beta = 2$, $\alpha\beta = 2$, from above giving $\alpha, \beta = -1 \pm i$. Hence $\#D(F_{2^m}) = 1 - ((-1-i)^m + (-1+i)^m) + 2^m$, and we have in one step the count of rational roots for all q^m , so for example

$$\#D(F_{1024}) = 1 - ((-1-i)^{10} + (-1+i)^{10}) + 2^{10} = 1 - (15 - 8i + 15 + 8i) + 1024 = 995.$$

Andre Weil extended this result to any algebraic variety V over $K = F_q$ through the Frobenius map $\pi_{V/K} : V \rightarrow V$, $x_i \rightarrow x_i^q$ whose fixed points are exactly the K rational points.

However this doesn't establish anything new about RH for the integer primes, because we

$$\text{simply get } \zeta_{\mathbb{Z}}(s) = \prod_p \zeta_{F_p}(s) = \prod_p \frac{1}{1 - p^{-s}}.$$